A Laboratory Study on the Influence of Guided Drop Tower Carriage Mass and Kinematic Differences to Full-Surrogate Free Falls Toward Enhanced Helmet Certification Methods

by

Aaron James Brice

B.Sc., University of Alberta, 2016

A Thesis Submitted in Partial Fulfillment of the Requirements for the Degree of

MASTER OF APPLIED SCIENCE

in the Department of Mechanical Engineering

A Laboratory Study on the Influence of Guided Drop Tower Carriage Mass and Kinematic Differences to Full-Surrogate Free Falls Toward Enhanced Helmet Certification Methods

by

Aaron James Brice

B.Sc., University of Alberta, 2016

Supervisory Committee:

Dr. Christopher Dennison, Supervisor

Department of Mechanical Engineering

Dr. Peter Wild, Departmental Member

Department of Mechanical Engineering

Dr. Joshua Giles, Departmental Member

Department of Mechanical Engineering

Abstract

Falling from height presents a significant risk for military personnel due to the frequency at which they perform high exposure maneuvers, such as walking along unstable structures, repelling from buildings or aircrafts, and low altitude egressing. Traumatic brain injury (TBI) resulting from falls from height (FFH) account for approximately 20% of TBIs with a reported cause in the military, despite the presence of protective head gear. This is likely because current certification testing performed on military helmets emphasize protection against ballistic threats over blunt impacts, such as falls. Military personnel have identified the need for the next generation of helmets to provide better protection against blunt impacts. To develop such helmets, a method for helmet evaluation in scenarios that are representative of real-life falls must be established as the new standard for helmet impact testing.

Guided vertical drop towers are a test device commonly used to evaluate the impact attenuating properties of protective headgear in headfirst falls during certification testing. These devices provide a simple, low cost, repeatable means for conducting certification tests over using full-body surrogates to replicate a person experiencing a headfirst fall. However, there are some limitations to the guided drop tower that may limit their ability to properly replicate a fall from height. The most notable limitations are that guided drop towers are constrained to only a single degree of freedom and the impact mass of a drop tower assembly typically only includes the mass of a human head and neck rather than the mass of a full-body. At present there is little work on how these limitations may yield a differing kinematic response between a guided drop tower and that of an actual fall. The objectives of this thesis was to determine if kinematic differences exist between a guided drop tower and a free-falling person, in unhelmeted and helmeted scenarios. The outcomes of this thesis will contribute toward the development of enhanced test standards that evaluate protective headgear in scenarios that are more representative of real-life falls.

A custom guided drop tower equipped with a Hybrid III head/neck and adjustable weight drop carriage along with a full-body Hybrid III 50th percentile male surrogate, to represent a falling person, were subjected to two experimental series 1) unhelmeted impacts at four angles between 30° and 75° and four impact velocities between 1.50 m/s and 3.00 m/s and, 2) helmeted impacts at 30° and 75° with impact velocities of 3.00 m/s and 4.50m/s. Impacts in both series were conducted onto a rigid impact surface and kinematic measures of head center of gravity linear acceleration, angular acceleration, and angular velocity were measured.

Results of the unhelmeted impact series identified that the drop tower can provide an acceptable approximation of the linear acceleration but not the angular velocity that is likely to be experienced by a person in a headfirst frontal impact. This is due to the angular velocity differing in either the magnitude of the peak angular velocity or direction and time instance of peak measures. Changes to the mass of the drop carriage, to be closer to that of a full dummy, did not bring angular velocity closer to that measured for the full dummy.

The helmeted impact study identified that a drop tower is likely to yield an underestimate of peak kinematics in shallow angle impacts and an overestimate of peak kinematics in steep angle impacts. This suggests that the drop tower, in its current form, provides a varying estimate of the resultant peak kinematics in helmeted impacts which is dependent on impact angle. These differences in response are primarily attributable to variances in helmet liner engagement when comparing the drop tower and a person falling.

The results of this research found that in their current form guided drop towers do not provide a true representation of the kinematic response that is likely to result in a headfirst fall, either unhelmeted or helmeted. Further the addition of mass to the drop carriage in either scenario did not alter the drop tower's response to a point where it matched the measured response of the falling surrogate .These differences in kinematic responses between the drop tower and what is likely to be experienced by a falling person, specifically in the case of underestimated responses in shallow angle helmeted falls emphasizes the need to further develop testing methods to ensure that future helmets are evaluated in a way that effectively tests the helmet's impact-attenuating abilities in an actual fall.

Contents

List of Figures

List of Tables

Preface

This research is an original work by Aaron Brice. Parts of this thesis will be submitted to be published in the Journal of Biomechanical Engineering.

This work was completed with a partnership in funding through the NSERC Alliance Grant and collaboration with Defence Research and Development Canada. The views and opinions expressed in this thesis are those of the author and do not necessarily reflect those of Defense Research and Development Canada or any of its employees.

Acknowledgments

I would like to first thank Dr. Christopher Dennison for taking the chance on someone who shared a common interest in riding dirt bikes. I truly appreciate your guidance and trust throughout the entirety of my graduate program and the opportunity to not only pursue this research freely but to also be so involved in setting up the Biomechanics and Instrumentation Lab for what will hopefully be many years of meaningful research.

I would also like to thank Simon Ouellet and Austin Azar of Defense Research and Development Canada for their support throughout my research.

To my extended colleagues Lindsey Agnew, Gaby Wynn, and Ashton Martin from the U of A I will always appreciate your help and friendship throughout everything along the way. From online classes in the middle of the pandemic, to transitioning to UVic, countless retests and thesis edits you all made this experience an enjoyable one.

There are so many other people that have helped me get here along the way that I would like to thank but the ones who have truly helped the most are my family. You have always encouraged me to challenge myself and have fully supported me every step of the way and for that I am beyond grateful.

Finally to Max, thanks buddy.

1.0 Introduction

1.1 Motivation

Traumatic brain injury (TBI) poses a significant health risk, with nearly 0.5% of the North American population experiencing some form of TBI each year [1] [2]. This amounts to approximately 1.7 million TBIs in the United States and 165,000 in Canada each year [1] [2]. Falls, slips, and trips are the most common cause of TBI, accounting for approximately 35% of TBIs reported in the US between the years 2002 – 2006. Fall-related TBI primarily occurs in pediatric (<14 years of age) and elderly (>65 years of age) populations, accounting for 47% and 20.5% of annual fall-related TBIs, respectively. For working age adults (ages 20 – 64), the primary risk for TBI is from automotive accidents and physical assault [1]. However, the risk of fall related injury for this age group is still present. Of the 523,043 fall-related TBIs reported between 2002 – 2006, 26% occurred in working aged adults which accounted for approximately 19.5% of TBIs reported in this age group [1].

The prevalence of TBI in military personnel is greater than that of the general population, as evidenced by the 4.2% of US service members who experienced TBI from 2000 – 2016. This high rate of TBI is likely attributable to military personnel often being tasked with high-risk maneuvers, such as walking along unstable structures, repelling from buildings or aircrafts, and low-altitude egressing, as well as exposure to events such as blasts, vehicle accidents, and assaults. Despite military personnel being equipped with protective headgear in such scenarios, falls are still a leading cause of TBI, representing approximately 20% of reported TBIs [3] [4]. This is likely because current certification testing performed on military helmets emphasizes protection against ballistic threats over protection against blunt impacts, such as falls [5], [6]. Military personnel have identified the need for the next generation of helmets to provide better protection against these forms of blunt impact while maintaining their ballistic protection. The first steps toward the development of such helmets is to thoroughly understand how current evaluation methods compare to real-life falls and what improvements can be made to these methods to achieve a better representation of a fall.

One way to develop this understanding is through the use of anthropometric test devices (ATDs), also known as crash test dummies, which are commonly used in injury research [7]. ATDs are designed with anatomical and mechanical properties that provide biomechanical responses similar to the human body. Used in conjunction with instrumentation, these devices provide repeatable kinematic responses from impact scenarios that are beyond a safe threshold for human volunteers [7], [8]. The Hybrid III dummy is a full-body surrogate model commonly used in blunt impact research to evaluate the influence of the body on head injury and helmet performance [7], [9], [10], [11]. Although full-body ATDs provide the best representation of real-life falls, they are often cost prohibitive and require a high level of test complexity which makes them impractical for use in helmet testing standards [7], [12].

Further, most helmet manufacturing facilities are equipped with drop towers, a simplified, lower cost form of test equipment that is used for certifying helmets across many helmet standards [13]. Drop towers use a surrogate headform that is either affixed to a carriage via a surrogate neck (guided impact) or a headform that is placed on top of a carriage with no mechanical connection (free fall impact) to simulate the impact energy of a scenario. The severity of the resultant impact is determined through kinematic measures, most commonly the resultant peak linear acceleration, which are compared against pass/fail criterion that a helmet must satisfy to be certified for use [14], [15], [16], [17], [18], [19], [20]. In both guided and free fall impacts, the carriage directs the headform from a fall height onto an impact surface. Both drop tower setups provide a repeatable method for evaluating fall impacts; however, guided drop towers are currently the most common test method used in helmet impact test standards [6], [13], [17], [19], [20], [21]. Although capable of producing repeatable impacts there are some limitations to the guided drop tower that may limit its ability to properly replicate a fall from height. The most notable limitations are that guided drop towers are constrained to only a single degree of freedom and the impact mass of a drop tower assembly typically only includes the mass of a human head and neck rather than the mass of a full-body [6], [13], [17], [19], [20], [21].

1.2 Research Objectives

Due to the impracticality of using full-body surrogates and the commonplace use of guided drop towers for helmet certification testing, it is preferable that new test standards for evaluating military helmets be designed for guided drop tower testing. To achieve this, it is necessary to first determine if a guided drop tower equipped with a Hybrid III 50th percentile head and neck and ballast mass can provide an adequate representation of a free-falling person, represented by a full-body Hybrid III 50th percentile male surrogate, in headfirst impacts. One of the objectives of this thesis is to use peak linear and angular kinematic data to determine whether differences exist between full-body and vertical drop tower impacts in unhelmeted and helmeted scenarios. A further objective of this work is to evaluate the effects of ballast mass on the resultant kinematics of a drop tower impact and to determine if the addition of this mass can achieve a closer approximation to full-body falls. The results of this study will be a first step towards developing new standards that evaluate military helmets for blunt impact protection in scenarios that are representative of real-life falls experienced by military personnel.

1.2 Thesis Organization

Chapter 2 provides the background information necessary for the work of this thesis. The chapter presents the kinematics and head injury metrics employed in injury biomechanics and their correlation to head and brain injury. The risks of fall related head injury are highlighted for both the general population and military personnel, as is the previous research conducted to understand the effects of the human body on headfirst falls. Existing helmet standards across sports and military are also discussed to show the differences that exist between them and to emphasize the need for improved military helmet testing standards.

Chapter 3 describes the equipment and experimental methods used as well as the analysis performed to determine the kinematics for the drop tower and dummy impacts.

Chapter 4 presents the findings for both the unhelmeted and helmeted impact series performed with the drop tower and full-surrogate and provides a comparison between the kinematics for the two series. Time curve comparisons are also presented to show how the components of the kinematics differ between the full-body and the drop tower.

Chapter 5 discusses the findings of the unhelmeted and helmeted series focusing on the kinematic differences between each drop tower configuration and the Hybrid III dummy and the implications of these differences. Finally, the limitations of this work are highlighted along with recommendations for future work to continue the development of a new impact standard for military helmets.

Chapter 6 summarizes the work of this thesis and its contributions.

2.0 Background Information

2.1 Traumatic Brain Injury

2.1.1 Definition of TBI

Traumatic and mild traumatic brain injury (TBI and mTBI) are forms of head injury, resulting from external forces acting directly or indirectly on the head, that cause a pathophysiological alteration in the brain [22], [23], [24]. There are two types of force that can act on the head and induce TBI, focal and inertial, which differ in the method in which they act upon the head. With focal forces, loading is applied directly to the head, which causes a localized deformation in the skull, or a pressure change within the brain [25], [26]. This form of loading typically results in moderate to severe TBI along with other injuries, such as skull fracture or hemorrhaging. Inertial forces result in tensile, compressive, and shear stresses that act on the brain, as a result of high rates of acceleration applied to the head, which are thought to be a primary contributor of mTBI. Inertial forces can be caused from either direct or indirect loading, but a combination of both of these loading scenarios is often observed [25], [27]. Focal and inertial forces can occur in scenarios of blunt impact in which the head contacts or is contacted by an object, causing localized direct loading that induces rapid motion of the head [2], [24], [28].

2.1.2 Mechanics of Brain Injury

The likelihood and severity of a brain injury is related to the translational and rotational motions that result from the inertial and contact forces that act on the head during an impact [29]. Indirect loading of the head results only in inertial forces, while direct loading, such as a head first fall onto a surface, induces both inertial loading and contact forces [25], [27]. Linear and angular accelerations that result from inertial loading and contact forces from an impact are mechanical measures that have been correlated to focal and diffuse injury risks. Impacts that act through a head's center of gravity (COG), meaning purely linear, are unlikely to result in a concussion [30]. For impacts that do not act directly through the head COG, which is more common in head impacts, both linear and angular accelerations occur. The resultant angular accelerations induce rotation of the brain which yields tensile, compressive, and shear forces of the brain tissue that

correlate to mTBI [30], [31], [32], [33]. Measurement of these kinematics is key to understanding the risk of TBI in falls.

2.1.3 Fall Related TBI

Falls typically occur between 3.5m and 10.5m (averaging 6.5m), and most commonly occur from ladders and windows (21% each) [34]. Headfirst impacts are the second most common orientation in a fall from height, after feet first, and result in an incidence rate of 60% for skull facture and nearly a 100% rate for cerebral damage [35]. Richter et al. found that the orientation of a fall is also a significant factor for survivability [34]. Clinical studies have reported that falls from a height greater than six meters, or roughly two stories, have a nearly 100% risk of injury [4]. Headfirst falls present an even greater risk, as a fall from a height of just one story has a fatality rate of ~50%; the fall height for individuals who strike feet first is 17.5m, which is consistent with the findings of Warner et al [34]-[35].

2.1.4 TBI in the Military

TBI is inherently present in the military with reports finding that an estimated 4.2% of all US service members between the years 2000 and 2016 experienced some form of TBI [3]. Among deployed service members, this rate is substantially greater with estimates ranging between 11 – 23% experiencing TBI [36], [37], [38]. Falls are among the leading causes of TBI in the military, representing approximately 20% of TBIs with a reported cause, despite the use of protective headgear which has been shown to reduce the severity of head injury from a fall [39], [40], [41], [42], [31]. The high-risk exposure to a fall induced TBI in military personnel is likely due to the execution of dangerous maneuvers, such as climbing over obstacles or walking along/on unstable or damaged structures. TBI is a significant risk for military personnel as it not only presents long-term health risks, but also has implications on the immediate safety of both a soldier affected by TBI and their fellow personnel. Individuals who are afflicted by TBI typically experience immediate physical symptoms, such as motor sensory impairment, dizziness, nausea, and blurred vision, in addition to cognitive impairments including a lack of attention, concentration, and perception [2], [24], [28]. A soldier experiencing these symptoms during military operations could present an increased risk of further injury to themselves or to personnel assisting the soldier[43], [44].

2.2 Head Injury Metrics

2.2.1 Head Kinematics

Peak linear acceleration (Peak G) is the most common measure for assessing head injury, as it is associated with the force impacting the head and relates to head injury severity [29], [45], [46], [47]. Although Peak G is a strong indicator of head injury severity, it cannot differentiate between different types of impacts such as impacts with rapid loading/unloading or impacts with long impact duration. These two impact scenarios may yield the same Peak G but due to the differences in how the loading is applied, the resultant injuries could differ significantly [47], [48]. Therefore, it is important to not only measure Peak G but to also consider the rate and directions in which acceleration is applied. Studies using cadaver, animal, and surrogate models have investigated how loading rate along with kinematic measures relate to injury severity [47], [49], [50], [51]. These studies have proposed mathematical injury metrics, such as the Head Injury Criteria (HIC) and the Diffuse Axonal, Multi-Axis, General Evaluation (DAMAGE) metric, that attempt to quantify the severity of the impact and the likelihood of injury occurring. These metrics have previously been defined and reviewed extensively [46], [49], [50].

2.2.2 HIC

The HIC was developed based on the limitations for linear acceleration impulse duration proposed by the Wayne State Tolerance Curve (WSTC) [49] and the Gadd Severity Index (SI) [47]. The WSTC was defined by fitting a curve to cadaver and animal test data results and establishes a threshold curve for linear acceleration versus impulse duration, for where skull fracture is likely to occur. For an acceleration and time duration that falls above the curve it is likely that skull fracture will occur while below the curve head injury may still occur, it is unlikely for there to be a fracture. The curve indicates that the linear acceleration that can be tolerated before skull fracture occurs decreases as the duration of the impulse increases [52] (Figure 1).

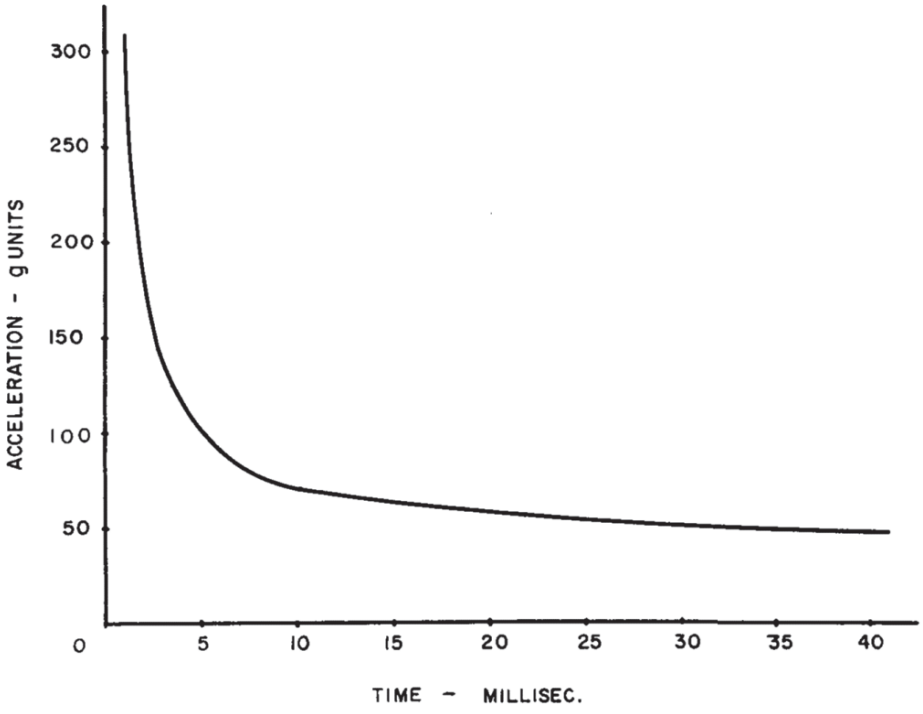

Figure 1: Wayne State Tolerance Curve for assessing head injury based on impulse duration. Accelerations that fall below the curve for a given time duration are considered likely to survive, while accelerations falling above the curve for a given time indicate a potentially fatal impact.

Figure reproduced with permission from Gurdjian, Elisha S., V. L. Roberts, and L. Murray Thomas. "Tolerance curves of acceleration and intracranial pressure and protective index in experimental head injury." Journal of Trauma and Acute Care Surgery 6.5 (1966): 600-604. (http://journals.lww.com/jtrauma/Citation/1966/09000/Tolerance_Curves_of_Acceleration_and_Intracranial.5.aspx)

The SI is a mathematical model, Eq. 1, that evaluates impacts over the entire duration of the impact and then assigns a risk of injury based from the equation [47]. The HIC, Eq. 2, is a modified version of the SI equation that limits the time over which the impact is evaluated to a specified time window [49].

$$SI = \int a^n dt \quad Eq. 1 \qquad \textit{Eq. 1}$$

Where: a = acceleration, n = weighting factor, t = time

$$HIC = \left\{ (t_2 - t_1) \left[\frac{1}{t_2 - t_1} \int_{t_1}^{t_2} a(t) dt \right]^{2.5} \right\}_{max} \qquad \textit{Eq. 2}$$

Where: a = acceleration, t = time

Several time windows for HIC have been proposed, however, HIC_{15} is the most common form of the HIC metric used to evaluate the risk of injury [53]. HIC_{15} determines the average linear acceleration impulse that occurs over a time window of 15 mS; the maximum average value from all of the evaluated time windows is evaluated as the HIC score. A HIC score of 1000 is defined as the limit for when head injury is likely to occur (i.e., a score of <1000 is unlikely to result in head injury, while a score >1000 is likely to cause head injury) [49]. Aside from being incorporated into HARM (Head Acceleration Response Metric) and HPS (Helmet Performance Score), there are few helmet standards that currently employ HIC as a pass/fail criterion [14], [48]. This is likely attributable to it adding a large amount of complexity into the determination of impact performance and only being useful in specific impact conditions [48]. Additionally, HIC does not include head rotational kinematics, and thus only considers the risk of serious injury such as skull fracture and not the risk of mTBI [54]. Despite the limitations of HIC and it not being widely used in helmet evaluation, it still provides a useful tool for comparing the effects and risks of head impacts. As such, it is used by many head injury studies [46], [51], [54].

2.2.3 DAMAGE

The Diffuse Axonal Multi-Axis General Evaluation criterion (DAMAGE) is a second order system that uses rotational head kinematics to predict resultant brain strains due to impact. The use of rotational kinematics, rather than linear acceleration, provides a better predictor for mTBI, as brain strain and subsequently diffuse injury, results from head rotation [29], [55]. DAMAGE was developed and validated computationally using a finite element model subjected to angular velocity inputs. Currently, the injury metric only provides a predictor for the resultant maximum principle strains due to an impact and not injury risk [50]. Despite not yet being correlated to injury risk, DAMAGE can still be used as an injury metric to evaluate impacts and helmet performance due to the correlations between brain strain and mTBI [50], [56].

2.2.4 Limitations of Peak Kinematics and Injury Metrics

Although peak kinematics and injury metrics provide a quantified means of evaluating the effects of the magnitude, rate of application, and duration of an impact, they may be unsuitable in comparative studies, The aforementioned response measures often depend on the resultant kinematics of an impact rather than the directional components of the kinematic data, meaning the directions in which the loading is applied is not considered. Thus, an impact to the side of the head may achieve the same peak kinematics and injury metric score as a frontal impact. Observation of the peak data and metrics from these two impacts would imply that they are equivalent when they are actually different impacts with potentially different injury risks. This is critical when comparing a drop tower and a full ATD impact or different impact locations; although the two impacts may achieve the same injury metric score, the means in which they achieve that score could be the result of different kinematics. To achieve equivalent impacts between impact types, given these potential differences in the kinematics, the directional components of the linear and angular kinematics should also be considered. `

Although this thesis only presents a subset of the many injury metrics that have been proposed for determining injury risk, they share a commonality with those not presented in that they use kinematic data to calculate injury risk [57]. if differences exist between the kinematic data of a full-body impact and a drop tower, the subsequently calculated amongst the many forms of injury metrics will also differ. Therefore, achieving equivalent kinematics between the two impact types is critical if injury metrics are to be considered as pass/fail criteria in future helmet evaluation methods that use guided drop towers.

2.3 Fall Injury Research

2.3.1 Surrogate Models

Anthropometric test devices, more commonly referred to as surrogates, are anatomical models that are designed to represent the human body. Surrogates are often employed in impact testing due to their many advantages compared to human volunteers and post-mortem human subjects (PMHS) such as being readily available and their ability to produce repeatable results at energies beyond injurious levels [8], [12], [58]. Surrogates can either be used purely for their anatomic attributes or be equipped with instrumentation, such as accelerometers and force transducers, to record kinematic and kinetic responses [8]. This instrumentation is typically housed within the surrogate model at key areas of interest for injury research such as the center of gravity (COG) of the head. This allows for direct measurement of the kinematics at the location of interest instead of relying on post processing transformations of data which is required when working with human volunteers and PMHS. As such, these surrogate models are able to provide insights on the mechanisms of injury that would otherwise not be measurable or have additional sources of error in the measurements [58]. An example of such a model is the Hybrid III, a full-body surrogate model (Figure 2). The Hybrid III is the standard model employed in frontal car crash testing and is often used in trauma biomechanics research [58], [59].

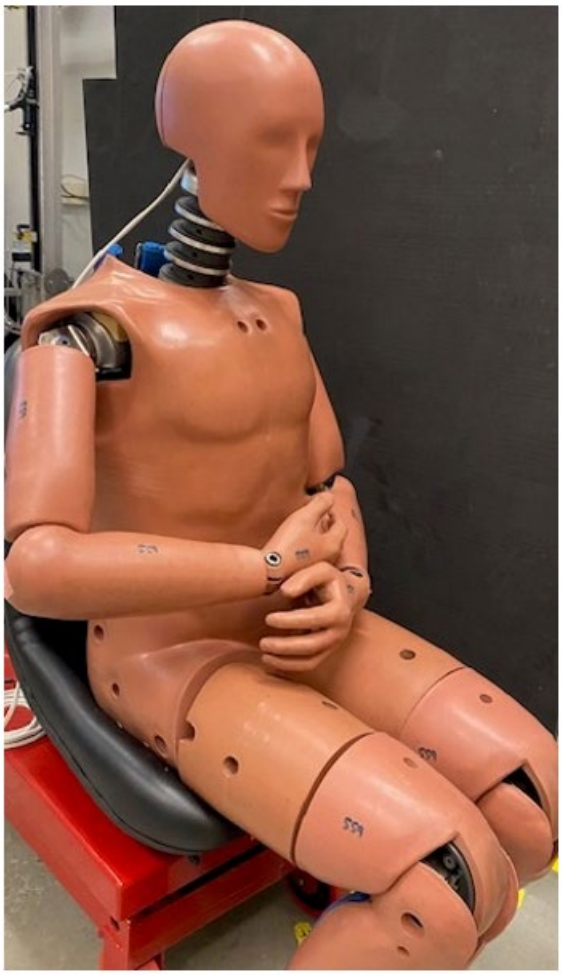

Figure 2: Hybrid III 50th percentile male model

Although surrogates provide many benefits, there are limitations and differences that exist between these models, human volunteers, and PMHS. Surrogates are typically constructed from common manufacturing materials like rubber, metal, and foam, which make them more economical as they are suitable for multiple impacts. To achieve this multi-impact durability, compromises are made in anatomical correctness; this includes using stiffer materials or using grossly simplified geometry of features, like solid circular segments to represent neck vertebrae. This is most notable for the Hybrid III neck, which has previously been shown to be too stiff and, as such, does not provide a truly biofidelic response to impact, where biofidelic is defined as a kinematic response that matches the response of a human [58]. Efforts have been made to make more biofidelic models compared to the Hybrid III model; however, the majority of these models

are still in their early development or are not yet commercially available [60]. Further, the Hybrid III is largely considered to be the gold standard in impact research due to the wealth of existing research that has previously been conducted with it which allows for direct comparison of results to other studies and injury reduction methods [56], [58], [59], [60].

2.3.2 Vertical Drop Towers

Vertical drop towers, which are common across most helmet test standards, are used to replicate a fall at a specified velocity onto an object that is either flat or some geometric shape [15], [16], [17], [18]. The configuration used in drop test standards can be classified as either a guided or free-falling impact. The primary difference between these configurations lies in how the headform is affixed to the test apparatus. In guided tests (Figure 3A), the headform is mounted onto a guide carriage via a neck surrogate, commonly a rigid aluminum post, that does not allow the head to move freely after impact [15], [16], [17], [18], [19], [20]. In free-falling tests (Figure 3B), the headform is either dropped completely free of any guide carriage or it is placed atop a guide fixture with no form of attachment, allowing for the head to move freely at the point of impact [14], [15], [16], [17], [18], [19], [20].

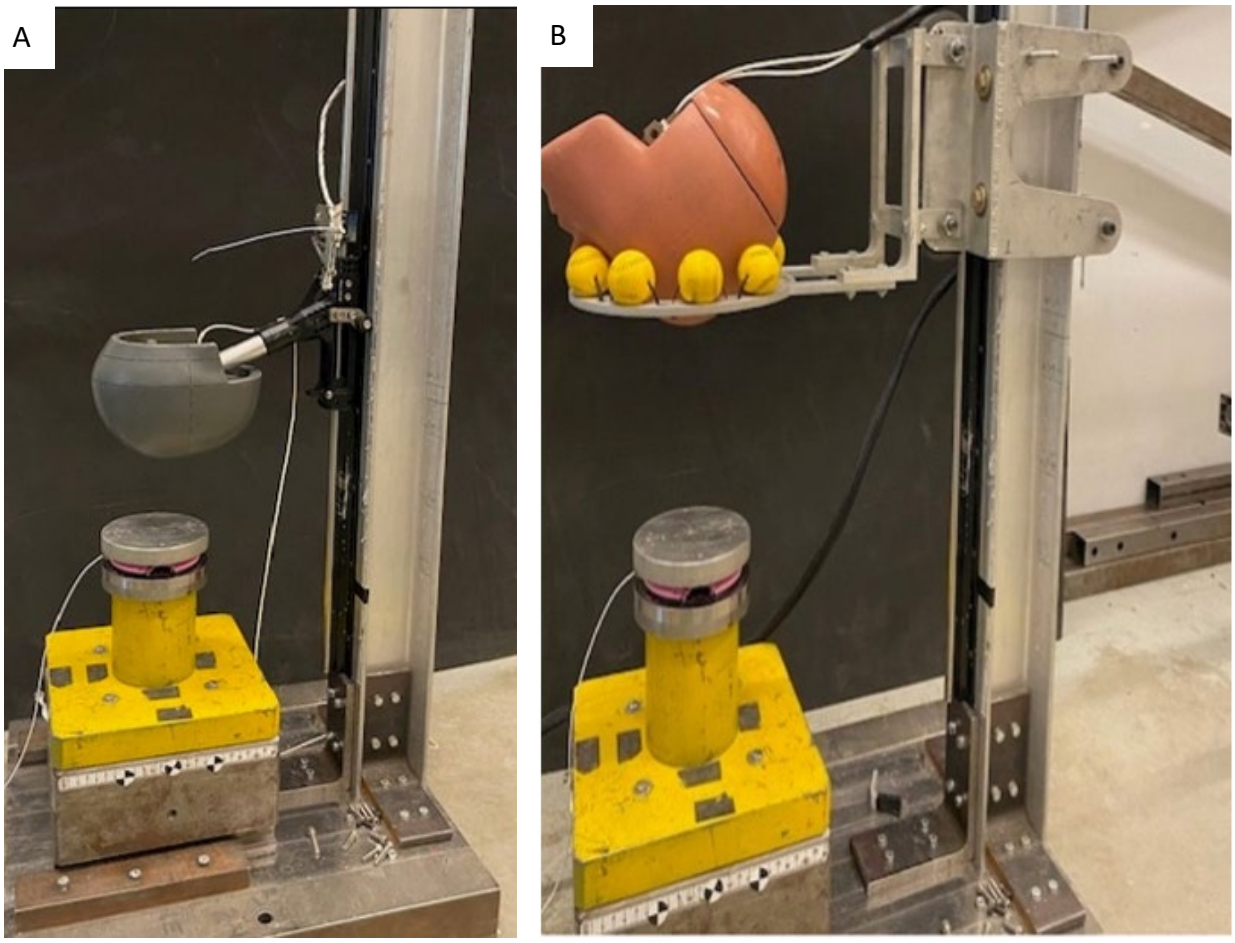

Figure 3: A) Example of a guided drop tower with a magnesium headform and rigid aluminum neck B) Example of a guided freefall fixture with a detached Hybrid III headform

Guided impacts that employ a rigid neck are the most common type of drop tower used in helmet testing. The use of a rigid neck prevents the ability to measure rotational kinematics as the surrogate head and carriage assembly are constrained to a single degree. This limits the drop tower's ability to match a real fall in which the head is able to rotate and produce the rotational kinematics that are associated with mTBI [61].

Drop towers that are used for research on head kinematics, mTBI, and helmet technology development typically use a drop assembly that has a non-rigid surrogate neck, such as the Hybrid III. These studies are often interested in further understanding how rotational kinematics influence head injury, therefore allowing for the head to rotate during impact is necessary [61]. However, these systems are often either a modified or custom-built drop system that do not have a standardized weight to the guide carriage [61], [62], [63], [64], [65].

2.3.3 Effective Mass Studies

The test equipment used for evaluating headgear performance should provide an equivalent impact to the event it is intended to simulate. To achieve this, an understanding of fall mechanics and the influence of the body in a fall event is needed. Experimental approaches using PMHS, and surrogate models have previously investigated how body mass influences the severity of resulting injuries and kinematics for varying orientations and impact surfaces.

Seidi et al. used 50^{th} percentile male and 5^{th} percentile female Hybrid III dummies to determine the effective mass in standing fall impacts onto a force plate. In frontal and rear impacts, they determined that the effective mass of impacts was equivalent to the mass of the head plus 47% and 49% of the neck mass for the male and female surrogate, respectively [11]. The effective mass for lateral impacts differed significantly, 22% for male and 6% for female. This can likely be explained by the findings of Ghajari et al., where they noted that the occipital condyle (OC) of the Hybrid III dummies does not provide a biofidelic representation in side impacts as it does not have the same degrees of freedom as a human OC [10].

Ghajari et al. also investigated how the presence of the body in impacts influences a helmeted impact both experimentally and computationally [10]. More specifically, they examined how helmet liner performance and head kinematics differ between full-surrogate impacts and isolated head impacts. Full-body impacts were performed using motorcycle helmets fit to a Hybrid III surrogate that was dropped in frontal, rear, and side impact orientations at 6 m/s. The results of the full-body impacts were used to validate a finite element (FE) model of the helmeted Hybrid III for comparison to isolated head impacts. FE results yielded a reduction in Peak g and an increase in head/helmet interaction forces when the body was present for flat anvil impacts. When evaluated at a velocity of 7.5 m/s, peak accelerations in the full-body impacts exceeded that of the isolated head, which was attributed to the helmet liner bottoming out in the full-body impacts, resulting in a spike in acceleration. To account for the influence of the body on Peak g, interaction forces, and liner compression, the researchers proposed the use of a weighted headform in isolated headform helmet testing. FE results of the weighted headform yielded a closer match to the results of the full-body results.

The COST327 action is an extensive investigation into the causes of head and neck injury to motorcycle riders [9]. Part of this investigation included experimental work on helmeted, headfirst full-body impacts and free-falling, helmeted headforms. The full-body impacts were conducted using a full Hybrid III pedestrian surrogate fit with a motorcycle helmet and aimed to understand how the mass and orientation of a rider's body alter the response of the head compared to a free-falling head. The surrogate was dropped in head-first falls onto flat and oblique abrasive anvils and compared to a free-falling helmeted headform subjected to the same flat anvil impact conditions. The dummy was dropped at impact angles of 0, 30 and 90 degrees, where 0 degrees was such that the body was parallel to the ground and 90 degrees was when the body was perpendicular to the ground. Impacts velocities were 4.4, 5.0, and 6.0 m/s. The results of this work showed that the kinematics between the full-body impacts and the isolated headform impacts were similar, but the headform required a higher impact velocity to match the rotational kinematics of the full-body. These findings suggest that if a free-falling headform is used for helmet standards, the test velocity needs to exceed the velocity that the helmet is actually intended for to accommodate for the lack of body mass. This work showed that the

presence of a neck and body mass does influence an impact relative to a free falling headform. However, it did not investigate guided tests in which a neck and guide carriage are present, therefore it does not explore if a higher impact velocity or ballast mass is also needed in guided impacts in order to match a free-falling full-body surrogate.

Despite the extensive work on understanding how the body influences injury severity and impact response, there is less investigation on potential differences that may exist between guided impactors and full-body impacts such as if ballast masses are required for guided impacts.

2.4 Helmets

2.4.1 Testing Standards

Helmets that are used in sports and recreation are regulated by testing standards to ensure they are fit for use and provide an acceptable level of protection to the user. These testing standards are defined based on the intended use of the helmet and may consist of several tests that the helmet design is required to pass. These tests can include vertical drops, projectile/ram impacts, retention/pull off tests, and environmental conditioning, among others. For drop tests and impact tests, the standards specify a certain level of impact energy that must be imparted onto the helmet, often via an assembly mass and impact velocity. For a helmet to be considered acceptable, it must attenuate the impact to below a specified threshold. Most commonly, this threshold is defined by an acceptable Peak g for a given impact velocity [14], [15], [16], [17], [18], [19], [20]. Examples of some common helmet certification standards are shown in table 1.

Table 1:Selected list of common helmet certification standards for single impact helmet types

Test Standard	Helmet Type	Configuration	Test Velocity (m/s)	Pass/Fail Criteria
FMVSS 218 [66]	Motorcycle Helmet	Guided monorail w/ magnesium headform and rigid aluminum neck, hemispherical impactor	5.2 6.0	<300 g peak linear acceleration
NOCSAE ND002-17m21[67]	Football Helmet	Cable Guided linear impactor w/ NOCSAE headform and flat impact surface, and pneumatic ram impact tester	3.46 5.47	<300 SI Score at 3.46 m/s <1200 peak SI score in all tests greater than 3.46 m/s <6000 rad/s^2
ECE 22.05[14]	Motorcycle Helmet	Free falling helmeted headform, flat and kerb stone impactors.	7.5	<275 g peak linear acceleration <2400 HIC
Snell M-2020[68]	Motorcycle Helmet	guided monorail w/ magnesium headform and rigid aluminum neck	7.9 8.2	<257g (size O@ 7.9m/s) peak linear acceleration <275g (size A @8.2 m/s) peak linear acceleration

Snell B-95[69]	Bicycle Helmet	guided monorail w/ magnesium headform and rigid aluminum neck	6.6	<300g peak linear acceleration
EN 1078[70]	Bicycle Helmet	Guided free fall	5.42	<250g peak linear acceleration
CANCSA–Z263.1[18]	Alpine ski Helmet	guided monorail w/ magnesium headform and rigid aluminum neck	5.40 +/- 0.16	<250g peak linear acceleration
EN 14572[71]	Equestrian	Guided free fall	4.4 7.7	<80g peak linear acceleration <250g peak linear acceleration
L1939SPEC Helmet Soldier[72]	Infantry Helmet (non-ACH)	guided monorail w/ magnesium headform and rigid aluminum neck	3.46 4.90	<150g peak linear acceleration
L1939SPEC parachutist[72]	Para Infantry Helmet (non-ACH)	guided monorail w/ magnesium headform and rigid aluminum neck	5.10 6.00	<250g peak linear acceleration
AR/PD 10-02[6]	ACH	guided monorail w/ magnesium headform and rigid aluminum neck, hemispherical impactor	3.1	<150g peak linear acceleration

2.4.2 Helmet Fit

The fit of a helmet on a user's head is also an important factor in helmet performance. Helmet fit is dependent on factors such as helmet position on the head, size relative to the user's head, and retention of the helmet in an impact. Correct placement of a helmet on a test headform is typically specified by the helmet manufacture and is commonly measured as the distance between the brim of the helmet and a reference line marked on the test headform used for a given standard. This distance is referred to as the Helmet Positioning Index (HPI) and is used to identify that the helmet is placed correctly. A common HPI reference is to have an approximately two-finger space between the brim of the helmet and the user's eyebrow. The significance of helmet fit and positioning was previously studied by Yu et al., where they evaluated how the fit and positioning of bicycle helmets altered resultant kinematics in falls [63].

2.4.3 Military Helmets

Military helmets are a single impact helmet that are designed primarily to resist penetration from ballistic projectiles. This is unlike other conventional single impact helmets, such as cycling or alpine helmets, which prioritize blunt impact attenuation [43].

Figure 4: Example of a modern military helmet

Even though military helmets emphasize ballistic protection, modern military helmets are still tested for impact attenuation using a modified version of a motorcycle helmet test standard for impact testing, FMVSS 218 [6], [73]. Impact testing consists of repeated impacts at 7 impact locations (Table 2) using an ISO standard headform fit with a military helmet, per the manufacturer's recommended HPI, and a rigid aluminum neck drop tower assembly.

Table 2: Impact locations used for impact testing on modern military helmets.

Impact Location	Orientation
Front	25 – 45 degrees from vertical
Rear	5 – 30 degrees from vertical
Left & Right Side	10-30 degrees from vertical
Crown	+/- 35 degrees from vertical
Left & Right Nape (Rear)	Rolled 15 – 30 degrees, 0 degrees off vertical

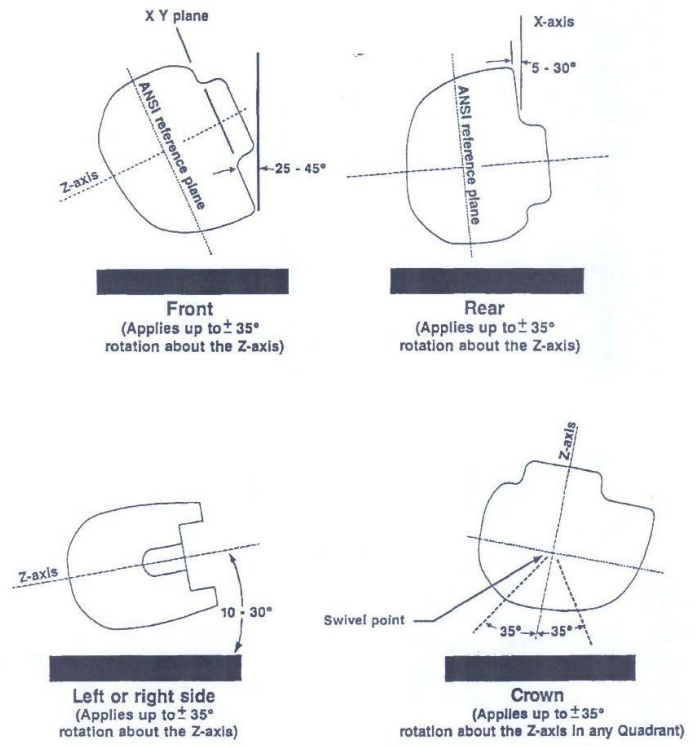

Figure 5: Impact orientations of the ACH helmet per ACH PD ar-pd 10-02[6]

The key modifications made to the FMVSS 218 test standard for the military helmet test are:

- Helmets are tested with a hemispherical impactor only.
- Each helmet is tested twice in each impact location.
- The successive impact is made between 1 and 2 minutes after the first impact.
- The test velocity for all impacts is 3.1 +/- 0.1 m/s.

Other modifications to the test standard include changes to the environmental conditioning, such as the omission of water emersion testing, and the padding configuration that is required within the helmet [6]. The helmet is tested with a standard 3/4" comfort liner and is fitted onto the standard headform that corresponds to the helmet size being tested per FMVSS 218. A helmet passes the impact testing requirement if no impact exceeds 150 g peak linear acceleration and it has no signs of physical damage, such as fracture, delamination, or compression of the shell which exceeds 0.15”.

The most notable modification to the test standard is the impact velocity and acceleration threshold. The impact velocity of the military helmet test was determined during the initial development of the modern helmet. Preliminary testing found that the helmets were able to yield a peak acceleration below 150 g at a velocity of 3.1 m/s, which was chosen as an acceptable level of performance and was subsequently adopted as the impact attenuation criteria [43].

The 3.1 m/s impact velocity used to test military helmets is equivalent to a free fall height of approximately 0.5m, which is substantially lower than what is likely to be experienced in theater. For example, a fall from a standing height of approximately 1.8m would produce an impact velocity between 6 m/s – 7 m/s [11] [74], while a fall from an increased height would yield even higher impact velocities.

3.0 Methods

This section describes the experimental equipment and test protocols used in this thesis. Additionally, it outlines the data analysis methods employed to compare the head COG kinematics of the weighted drop tower and free fall impacts.

3.1 Experimental Equipment

3.1.1 50th Percentile Hybrid III Surrogate

A full body Hybrid III 50th percentile male surrogate model (Figure 6A) (Humanetics, Farmington Hills, MI, Standard ATD 78051-218-H) was used in free falling surrogate experiments, as described in Section 3.1.2, while an isolated Hybrid III head and neck were used in drop tower experiments, outlined in Section 3.1.3. For full-body free falling experiments, the Hybrid III neck was fixed to the torso and set in the 0° position on the neck mounting block, as shown in (Figure 6B).

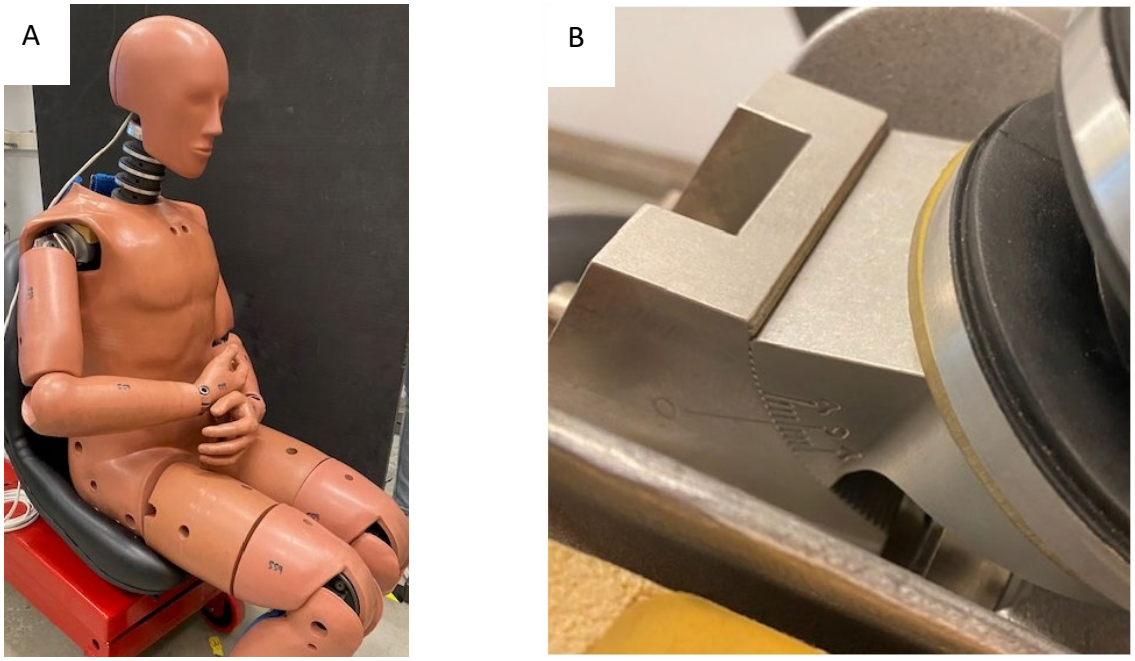

Figure 6: A) 50th percentile Hybrid III male surrogate model B) neck mounting bracket position

Instrumentation for the Hybrid III headform consisted of a nine uniaxial accelerometer array (Measurement Specialities Inc., Hampton VA, model 64C-2000-360) mounted inside the head using a 3-2-2-2 configuration; three accelerometers at the head centre of gravity (COG), and two each at the crown, front, and left side. Data was acquired at a sampling frequency of 100 kHz and initially processed with an anti aliasing hardware filter applied to the analog voltages with a 4 kHz corner frequency. This was achieved with a data acquisition system (DAQ) using custom amplifiers set to 64 dB gain for the accelerometers and 128 dB for the upper neck load cell, two DAQ cards (PX1 6251, National Instruments, Austin TX), and LabView software (LabVIEW v8.5, National Instruments, Austin TX). The head acceleration data was post processed in MATLAB R2020b (MathWorks Inc., MA United States) with a 4th order Butterworth filter at a cut-off frequency of 1650 Hz, per Channel Frequency Class 1000 (CFC1000). The sampling rate and filtering method were selected in compliance with the SAE J211 standard for instrumentation in impact tests [75]. Linear head COG accelerations were determined directly from the filtered accelerometer data. Angular accelerations and angular velocity were mathematically determined via equations proposed by Padgaonkar and integration of angular accelerations, respectively [76].

The coordinate system used to determine head kinematics is defined per the SAE J211-1 standard, shown in (Figure 7).

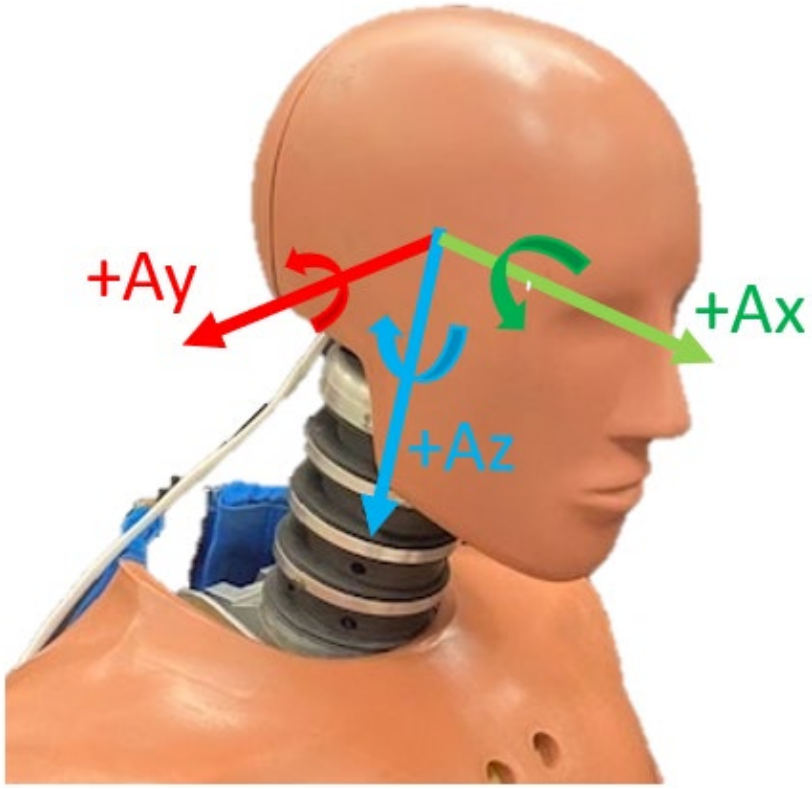

Figure 7: Hybrid III headform with the positive coordinate system of the head COG accelerations shown. The X-axis corresponds with the sagittal axis (green), the Y-axis with the frontal axis (red), and the Z-axis with the longitudinal axis (blue).

3.1.2 Free Falling Full Body Surrogate Experiments

For free falling experiments with the full Hybrid III dummy, the dummy was rigged in a prone position using two adjustable lifting straps; one on each shoulder joint and a turnbuckle attached to both legs just above the knees. The straps were connected to links attached to a lifting device consisting of a shackle, eye bolt and steel block. The lifting device was attached to a hoist by a magnetic release (Figure 8A). The straps could be adjusted to orient the dummy at a desired impact angle. To achieve a shallow angle measured relative to the impact ground and the longitudinal axis of the body, the shoulder straps were shortened, and the turnbuckle lengthened. Similarly, for a steep impact angle, the shoulder straps were lengthened, and the turnbuckle shortened.

The independent shoulder straps allowed the dummy to be rotated about its longitudinal axis to ensure that the shoulders were level with each other prior to release. This was determined by aligning each shoulder relative to a laser level (Figure 8B). This ensured that the dummy fell without rolling to one side due to a mass imbalance caused by the body being misaligned prior to release. The dummy used in this work features a molded pelvis that is primarily intended for frontal car crash testing which naturally conforms to a seated position rather than a standing position. To compensate for the dummy's tendency to relax to a seated state, a strap running along the dummy's back was added between the upper legs and the mid point between the shoulders.

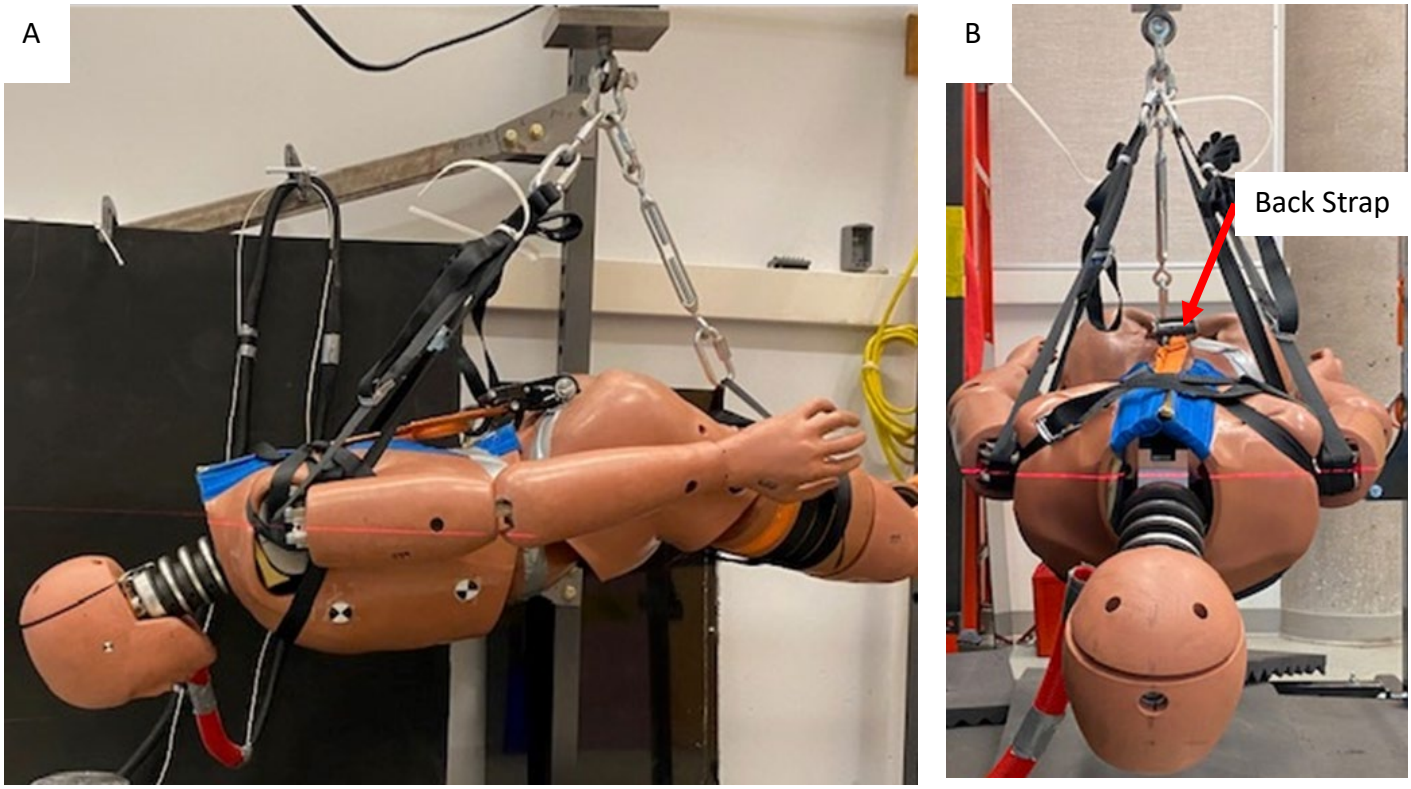

Figure 8: A) Rigging system used for lifting and positioning the dummy at the desired impact angle. B) Laser line across shoulders ensures flat dummy positioning to prevent rolling during freefall.

The shoulder, elbow, and knee joints were locked out to prevent them from inducing any undesired rotation or movement. The arms were positioned straight along the side of the body to ensure that they did not contact the ground or impact surface prior to or during head impact. The configuration used for this work is similar to that of the COST327 study conducted by Hering et. al.[77].

The dummy was lifted to the height corresponding to the desired impact velocity. To ensure repeatable impact velocity across any test angle, the height that the dummy was released from was measured as the distance from the impact surface to the head COG of the headform, as indicated by a target positioned on the side of the head. The drop angle was defined as the angle of the neckline measured immediately prior to release which was measured using an angle finder placed on the neck (Figure 9).

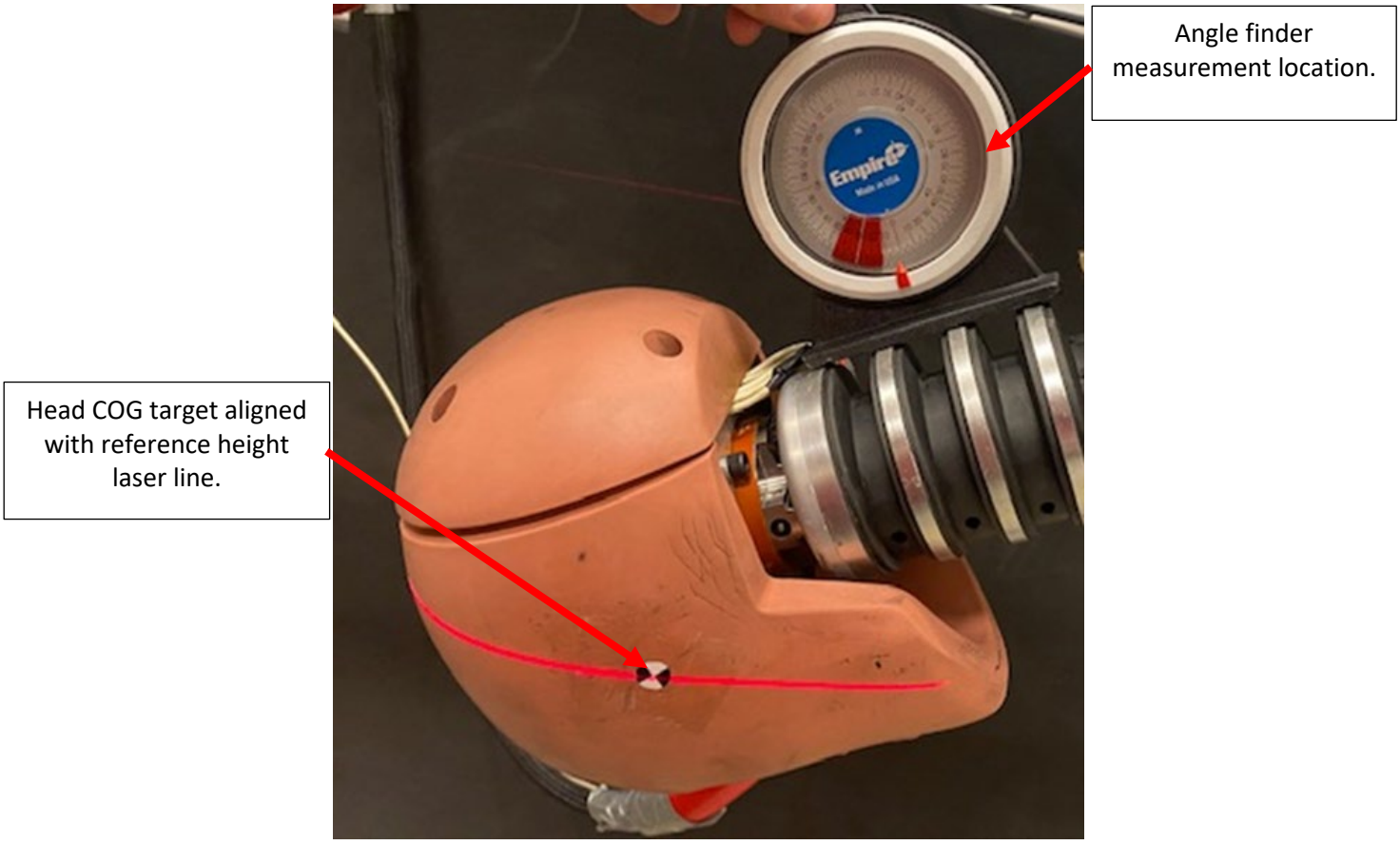

Figure 9: Pre-drop height and angle verification of the hybrid III head and neck just prior to release

Once the dummy stabilized after being raised, the shoulder alignment, release height, and drop angle were checked immediately before release. The surrogate then fell freely, headfirst, onto the impact surface before landing on a foam pad placed below the body.

3.1.3 Vertical Drop Tower and Gimbal Assembly

A custom assembly consisting of the same 50th percentile male Hybrid III head and neck used on the dummy, section 3.1.1, was assembled onto a drop carriage on a linear rail (Figure 10) for use in the vertical drop tower impacts described in sections 3.2 and 3.3. The carriage is designed with a gimbal that allows the head and neck assembly to be positioned at a desired drop angle from 0° to 90°, as well as rotated about the z-axis to achieve multiple impact angles. The drop carriage is mounted to the vertical beam via a linear bearing and guide rollers. Two sets of wheels along the back of the beam are used to ensure stability during free fall.

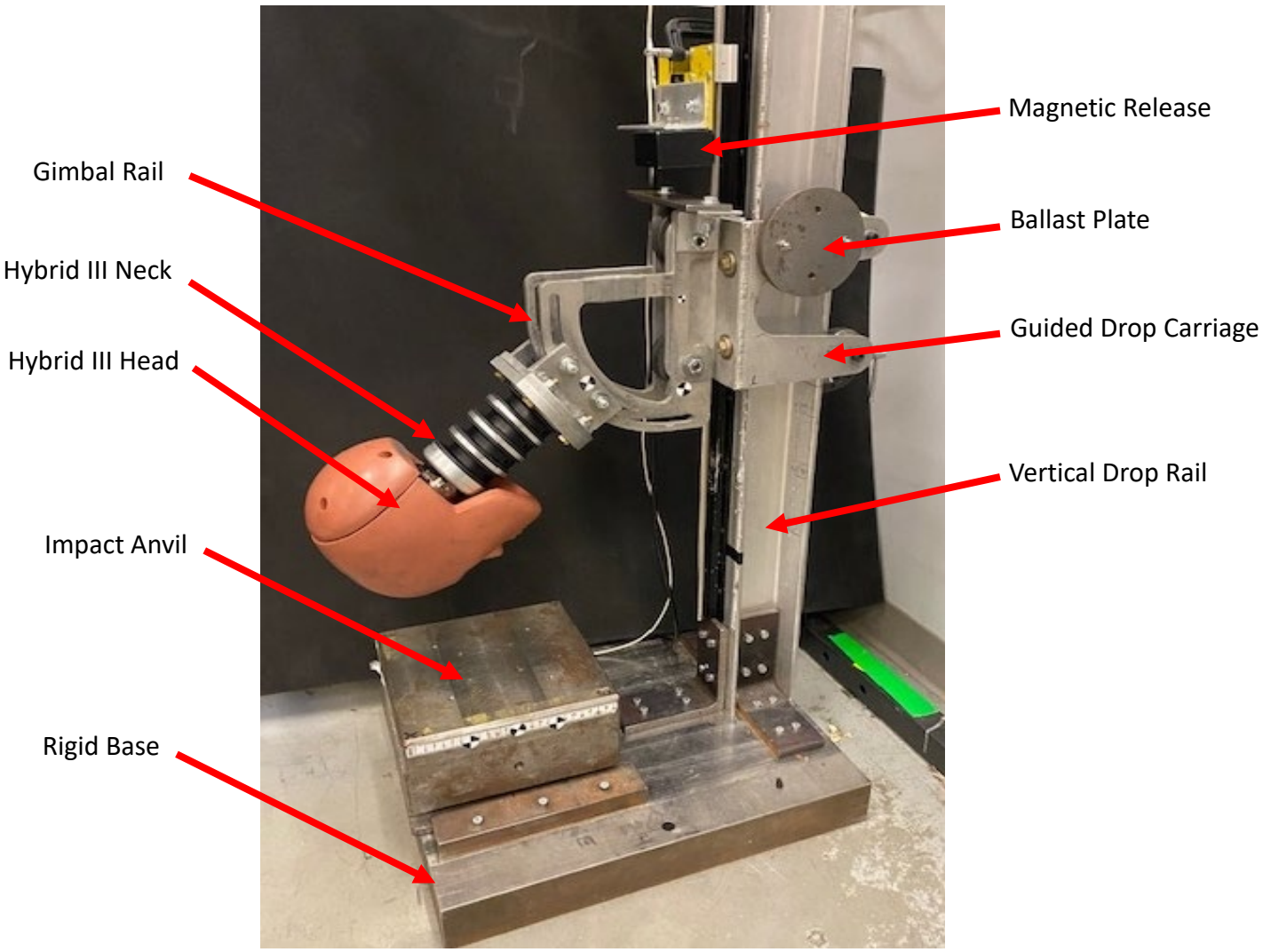

Figure 10: Vertical drop tower system fitted with Hybrid III head/neck and custom drop carriage.

The mass of the carriage when fitted with the head and neck is 11.75 kg. The carriage can also accommodate up to 6 ballast mass plates, each weighing approximately 1.24kg. Plates are added in increments of 2 plates to keep the carriage balanced, which allows for 4 assembly masses (Table 3).

Table 3: Mass of the drop carriage assembly, including Hybrid III head and neck, by the number of ballast plates.

Number of Ballast Plates	Carriage Assembly Mass (kg)
0	11.75
2	14.22
4	16.70
6	19.17

The impact anvil consists of a moveable flat steel block placed on top of a stationary base (Figure 10, above). The base is used to mount the vertical rail and provides additional mass. The flat steel block acts as the impact surface and can be moved along the stationary base to achieve the desired impact location of the head for the chosen impact angle. Once positioned, the block is clamped to the base with two clamping bars to provide a rigid impact surface. The use of a flat impact surface is common amongst many helmet testing standards [78]. The drop carriage is released from an adjustable magnetic release at predetermined heights to overcome any rolling resistance of the guide wheels and achieve the desired velocity at impact. The height that the fixture is released from, and the pre-release neck angle are measured using the same method as described in section 3.1.1. Once the release height and neck angle were verified, the carriage fell along the guide rail and the headform struck the impact surface.

3.2 Unhelmeted Impact Protocol

An experimental series with four impact angles and four impact velocities was conducted for both a Hybrid III 50th percentile male full-body surrogate and an isolated Hybrid III head and neck, fixed to a vertical drop tower and configured with four ballast masses, in a frontal impact orientation. A frontal impact (Figure 10, above) was selected as this is a common impact location used in helmet testing certifications [6], [66], [68], [79]. Other impact locations, such as oblique and side, were considered; however, due to limitations in the rigging of the full-surrogate and inability to ensure repeatable free falls in these configurations, they were omitted in this work. The impact angles selected for impact were as shown in Table 2.

Table 4: Impact angles for full-surrogate and drop tower impacts unhelmeted test series

Impact Angle
30°
45°
60°
75°

A 30° impact angle was initially selected since it falls within the acceptable range of angles to represent a frontal impact in the current military helmet testing specifications, as described in Table 3. The other three impact angles were chosen at 15° increments up to 75°, which still fall within the acceptable range of the military helmet crown impact tests [6].

Table 5: Acceptable impact ranges for a military helmet impact test in frontal and crown tests

Impact Location	Orientation
Front	25° – 45°
Crown	55° – 125°

A 10° impact angle was considered, which was intended to replicate an approximately 0° impact without impacting the nose first. However, due to rotation and slip of the head along the impact surface in the 10° configuration, the nose of the surrogate was damaged. As such, it was decided to not continue with this impact orientation to prevent further damage to the head. 90° impacts were also considered but due to interference between the headform and the drop tower, the 90° configuration was also omitted.

A requirement to not exceed a peak acceleration of 300 g, to avoid damage to test equipment or dislodging of any sensors, also limited the unhelmeted impacts to a maximum of 3.25 m/s. This maximum impact velocity was determined through a pilot series using the drop tower. The headform was dropped from incrementally higher fall heights, beginning at 20cm, for each angle and impact mass.

After each configuration was tested, the fall height was moved up by 20 cm and the tests were repeated until a acceleration of ~300 g was achieved for any test in one of the configurations. A Peak g of 317.55 g occurred at a configuration of: 80 cm fall height, 75° impact angle, and 19.2 kg carriage mass. This configuration corresponded to an impact velocity of ~4m/s.

After completing the pilot study, four target impact velocities were chosen for the primary study (Table 6).

Table 6: Velocities for full-surrogate and drop tower impacts unhelmeted test series

Impact velocity (m/s)
1.50
2.00
2.50
3.00

It should be noted that the upper end test velocity matches current military helmet test velocities but falls below the impact velocities that are commonly specified in other helmet standards and the average velocity that results from falls from heights [80], [81], [82].

Due to the lack of the presence of a helmet in this portion of the study, it was not possible to achieve the higher test velocities of other helmet standards without risking damage to the sensor array. The use of a helmet was omitted as the main objective of this series was to identify what differences, if any, exist in the head kinematics between a drop tower and a full-surrogate, and the use of helmet may have confounded these results as previously shown by Hering et al. [77].

3.3 Helmeted Impact Protocol

Helmeted impacts with the drop tower and the full-body surrogate were conducted in the same manner as the unhelmeted tests in 30° and 75° configurations. Two drop tower weights were used for the helmeted impacts: 11.75 kg and 19.20 kg. A total of eighteen helmets were tested: twelve on the drop tower and six on the full-surrogate. Each helmet was impacted once in two locations: frontal (30°) and crown (75°). Two velocities, 3.0 m/s and 4.5 m/s, were used. A test velocity of 6.0 m/s was considered in order to be consistent with FMVSS 218 [73], the standard that military helmet impact tests are based on. However, 4.5m/s was the maximum velocity that could be achieved due to limitations on the height of the hoist. Three impacts were performed at each velocity, angle, and weight for a total of 36 helmeted impacts.

Helmet position was set such that the brim of the helmet was 74 mm from the bottom of the nose (Figure 11). This distance between the brim and the helmet was chosen as it corresponds to the same HPI on a Hybrid III head as the HPI for the military helmet on a test headform. This position was measured prior to each drop with a digital caliper. The retention system was tightened against the head once the brim distance was set. As there were no fit force sensors on the headform, the retention system was tightened based on feel by turning the adjuster dial until it was finger tight and then an additional 1/8 turn was added. Finally, the chin straps were adjusted to even lengths on both sides of the head and were set so that there was no slack in the straps. This method of helmet fit is based on the recommended fit for military helmets [6].

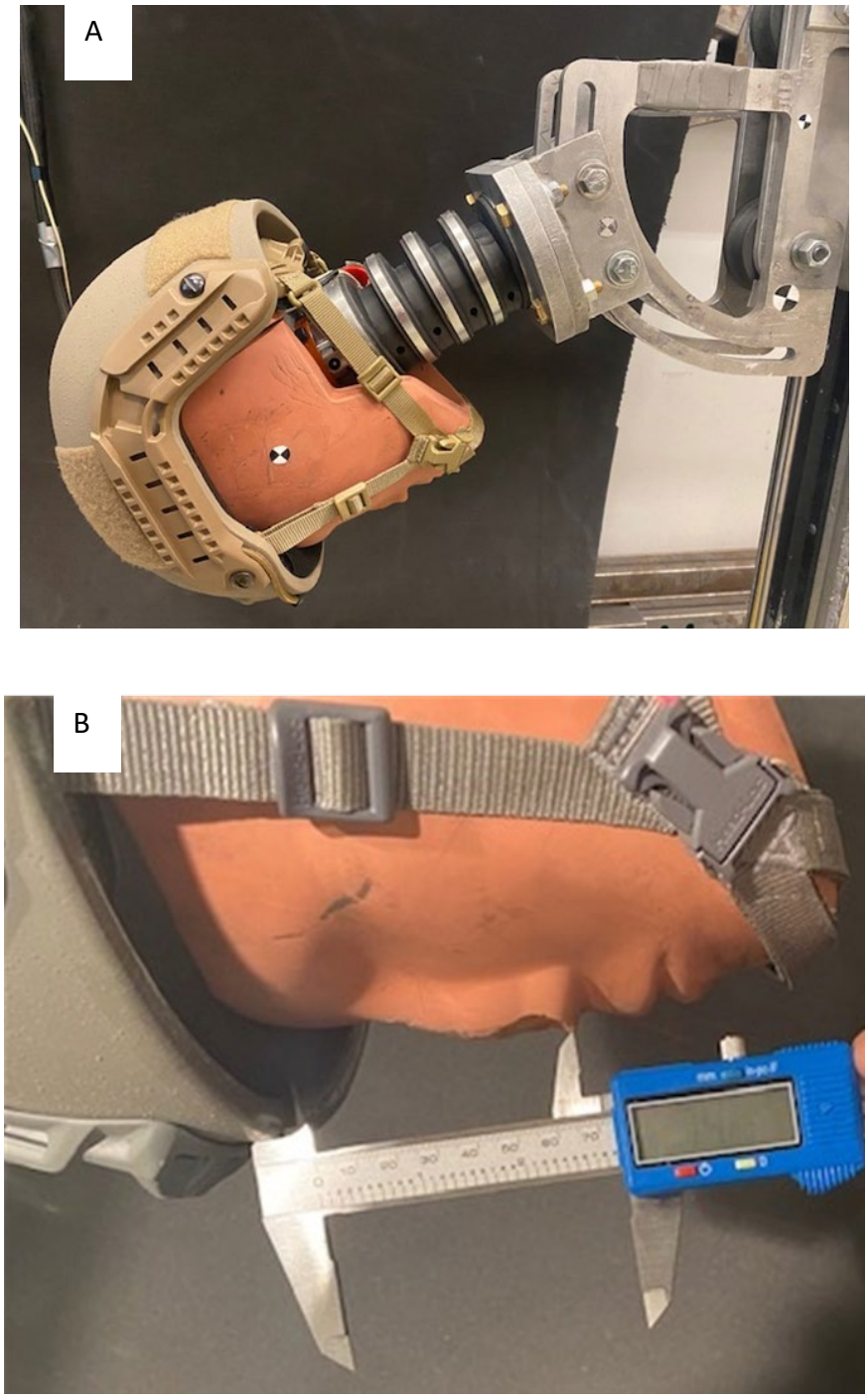

Figure 11: A) Placement of a military helmet onto the Hybrid III headform with correct placement between the nose and helmet brim per the HPI for a military helmet test. B) measurement of the 74mm between the nose and the helmet brim to achieve the correct HPI.

3.4 Data Analysis

3.4.1 High-Speed Video Analyses

To capture impact speed and impact angle, a high-speed camera (Phantom v611, Vision Research, Wayne NJ), equipped with a Carl Zeiss (Jena, Germany) 50mm f/1.4 macro lens, was used at a recording speed of 5000 fps (Figure 12). The camera was calibrated prior to recording impact data by determining the number of image pixels that correspond to a distance of 101.6mm along a ruler placed in the plane that the measurements were to be taken.

Figure 12: Placement of high-speed camera for full-body impacts to allow for measurement of angle and velocity at impact.

Impact speed was calculated using the Phantom CineViewer Software (v3.4, Vision Research, Wayne NJ) by determining the displacement of a high contrast tracking target placed at the head-neck junction in the video captured by the camera perpendicular to the principal plane of motion. To determine the impact velocity, the center of the velocity target was identified 10 frames prior to the frame in which impact occurs. The center of the velocity target was then located in the frame just prior to impact. After identifying these two points, the CineViewer software calculated the velocity using the displacement distance, based on the number of pixels that the target has moved, and the time between the two measurement frames.

Impact angle was determined in CineViewer using the frame just prior to impact by drawing two lines, one along the neckline and a second along the edge of the impact anvil, as depicted in (Figure 13)

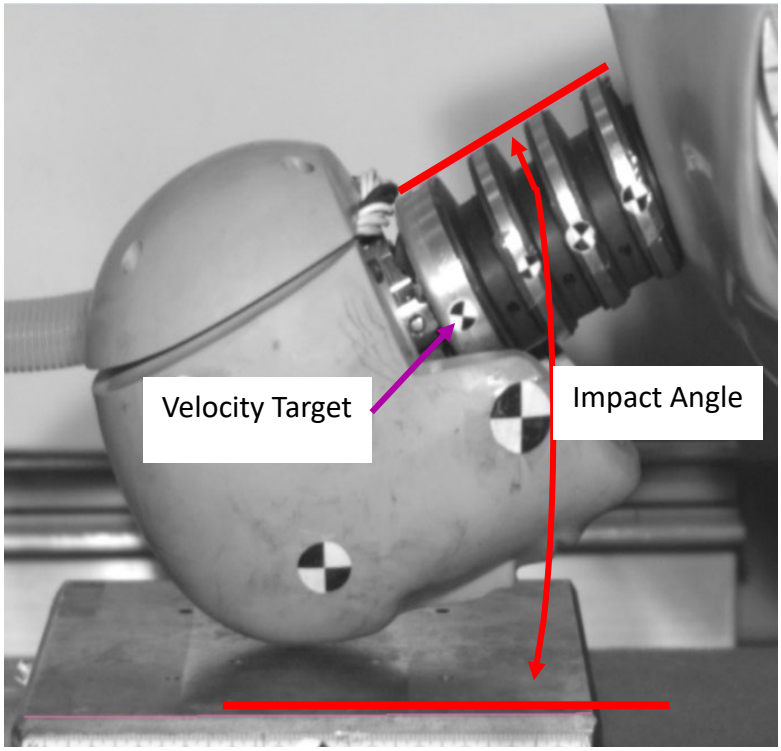

Figure 13: High Speed video frame just prior to impact for a 30-degree full-surrogate impact indicating the velocity target, and angle measurement reference lines.

3.4.2 Statistical Analyses

All statistical analyses were performed using IBM SPSS Statistics V29 (Armonk, NY). A significance of $p<0.05$ was used. Mean values and standard deviations (SD) for head COG linear acceleration, angular acceleration, and angular velocity, along with impact velocity and impact angle measurements were analyzed for all recorded impacts using multiple analysis methods to determine if differences exist between the mean peak kinematics of the full-body impacts and the drop tower impacts.

Time series comparisons of the components of the head COG kinematics were performed to determine if the peak kinematics and injury metrics are a product of equivalent impacts or, if not, to understand where the differences exist between the two impact scenarios.

For unhelmeted impacts, the effect of additional mass added to the drop tower and the statistical significance between each test mass and the Hybrid III free-falls were grouped and compared by impact angle. For example, the mean kinematics for each mass configuration and test velocity for the 30° impacts were compared against each other, but not compared against the mean kinematics of other impact angles. This method of evaluating each angle separately was chosen because the objective of this work was to determine how much additional mass may be required on a drop tower carriage to match a free-fall impact at a given angle. Therefore, maintaining a consistent mass across all impact velocities for a given angle was considered a requirement, but it would be acceptable to have differing drop tower masses for different impact angles. For helmeted impacts, the data sets were grouped by angle and impact velocity. This additional grouping by velocity was chosen as the influence of helmet liner engagement on resultant kinematics was anticipated to differ significantly between both the impact angle and impact velocity [9].

4.0 Results

This chapter compares full-surrogate and drop tower kinematics for both unhelmeted and helmeted impacts. Further, the influence of multiple ballast masses on the kinematics of a drop tower are summarized.

4.1 Unhelmeted Impact Results

A summary of the mean impact angle and associated SDs are reported in Table 7 for each unhelmeted impact configuration of the full-body and drop tower experiments. Means for Peak g, Peak α, and Peak ω of the unhelmeted impacts are summarized for each impact angle and reported in Table 7 – Table *10* as mean ± standard deviation. Head kinematics are reported as the peak resultant value of the X, Y, and Z components.

Table 7: Mean Impact Angle and Standard Deviation for Drop Tower and Full-Surrogate (78.00 kg) in Unhelmeted Impacts by Target Angle and Velocity for Each Carriage Mass.

		Drop Tower Mass (kg)								Full-Body (kg)	
		11.75		14.22		16.70		19.17		78.00	
Target Angle	**Target Velocity (m/s)**	**Mean Angle**	**Std. Dev**	**Mean Angle**	**Std. Dev**	**Mean Angle**	**Std. Dev**	**Mean Angle**	**Std. Dev**	**Mean Angle**	**Std. Dev**
30°	1.50	27.1	0.6	26.8	0.5	26.8	0.5	26.8	0.2	30.1	1.2
	2.00	27.4	0.2	27.3	0.3	27.1	0.6	26.8	0.4	30.0	0.7
	2.50	27.5	0.3	27.6	0.3	27.6	0.1	28.1	0.4	29.3	0.7
	3.00	28.9	0.7	27.2	1.5	25.9	0.7	26.1	2.2	30.0	0.8
	Overall	**27.7**	**0.7**	**27.2**	**0.3**	**26.8**	**0.7**	**27.0**	**0.8**	**29.9**	**0.3**
45°	1.50	43.1	0.3	42.8	0.6	42.8	0.7	40.6	0.2	44.2	0.5
	2.00	42.2	0.2	41.2	0.3	41.2	0.1	42.6	0.7	42.5	1.3
	2.50	42.4	0.3	42.2	0.4	41.7	0.2	41.6	1.2	44.2	1.2
	3.00	42.6	0.4	42.7	0.4	42.3	0.3	41.9	0.3	43.7	1.8
	Overall	**42.6**	**0.3**	**42.2**	**0.6**	**42.0**	**0.6**	**41.7**	**0.7**	**43.6**	**0.7**
60°	1.50	54.7	0.1	54.4	0.2	54.6	0.2	54.9	0.4	57.9	0.8
	2.00	54.3	0.4	54.4	0.5	55.0	0.2	54.7	0.5	56.4	0.7
	2.50	55.1	0.5	55.2	0.5	54.9	0.2	54.6	0.1	57.0	1.2
	3.00	58.7	0.3	58.3	0.3	56.7	0.9	54.4	0.7	57.5	0.7
	Overall	**55.7**	**1.8**	**55.6**	**1.6**	**55.3**	**0.8**	**54.6**	**0.2**	**57.2**	**0.6**
75°	1.50	71.9	0.2	72.2	0.2	72.4	0.3	72.3	0.3	73.9	2.0
	2.00	71.4	0.4	72.2	0.9	72.4	0.2	72.3	0.2	73.7	0.9
	2.50	71.2	0.3	71.6	0.7	72.3	0.3	72.2	0.1	72.4	0.6
	3.00	71.5	0.4	72.1*	0.7*	72.9	0.2	72.5	0.3	72.7	0.3
	Overall	**71.5**	**0.3**	**72.1**	**0.3**	**72.5**	**0.3**	**72.3**	**0.1**	**73.2**	**0.6**

***Outlier removed: N = 4, for 75-degree, 14.22 kg, 3.00 m/s impact configuration**

Table 8: Mean Peak Linear Acceleration and Standard Deviation for Drop Tower and Full-Surrogate (78.00 kg) in Unhelmeted Impacts

		Velocity (m/s)							
		1.50		2.00		2.50		3.00	
Drop Angle	Weight (kg)	Mean Peak G	Std. Dev.	Mean Peak G	Std. Dev.	Mean Peak G	Std. Dev.	Mean Peak G	Std. Dev.
30°	11.75	93.0	2.3	138.3	4.9	172.1	1.6	228.4	4.261
	14.22	96.2	0.6	147.8	1.0	179.0	3.5	241.6	4.6
	16.70	97.8	1.1	152.8	1.2	185.1	1.2	256.7	4.3
	19.17	99.3	1.4	154.2	1.4	180.5	5.9	253.2	5.8
	78.00	83.6	2.4	137.7	2.1	186.4	2.2	264.9	2.7
45°	11.75	81.9	1.9	90.7	2.7	164.2	1.2	248.8	9.3
	14.22	85.8	1.4	90.7	2.8	167.6	1.2	256.5	3.7
	16.70	86.4	1.3	89.1	0.5	173.0	2.4	259.8	2.4
	19.17	84.2	1.4	89.1	1.7	173.7	3.4	264.1	1.3
	78.00	70.7	1.2	125.1	2.3	171.5	1.7	249.1	2.8
60°	11.75	80.0	0.8	125.1	1.8	170.1	1.3	250.0	3.6
	14.22	83.0	2.2	130.2	1.5	176.7	1.3	260.4	2.1
	16.70	81.7	0.7	131.8	1.5	181.1	1.2	269.6	3.4
	19.17	83.4	0.5	133.8	1.0	180.6	3.6	275.9	2.7
	78.00	65.6	2.0	123.3	2.2	172.8	2.2	265.9	4.3
75°	11.75	74.9	0.6	109.2	0.9	149.7	3.4	229.3	1.0
	14.22	77.7	0.9	113.0	1.6	157.6	1.7	246.4*	9.3*
	16.70	79.7	0.7	116.3	0.9	161.9	2.3	255.7	1.2
	19.17	80.2	0.3	118.9	1.0	164.2	1.0	261.5	1.7
	78.00	64.7	3.8	119.9	1.8	166.1	2.2	255.3	2.4

***N = 4, for 75-degree, 14.22 kg, 3.00 m/s impact configuration**

Table 9 Mean Peak Angular Acceleration and Standard Deviation for Drop Tower and Full-Surrogate (78.00 kg) in Unhelmeted Impacts

		Velocity (m/s)							
		1.50		2.00		2.50		3.00	
Drop Angle	Weight (kg)	Mean Peak α	Std. Dev.	Mean Peak α	Std. Dev.	Mean Peak α	Std. Dev.	Mean Peak α	Std. Dev.
30°	11.75	4284.0	135.4	6686.3	221.5	8131.5	170.6	10996.1	360.3
	14.22	4445.9	51.5	6996.4	201.5	8527.5	217.3	11937.6	289.3
	16.70	4501.7	58.7	7138.7	116.2	8772.7	110.9	12383.4	190.2
	19.17	4574.3	52.2	7193.3	97.2	8455.8	374.8	12450.6	287.4
	78.00	3507.3	114.1	5859.1	217.7	8352.7	159.2	12537.4	170.5
45°	11.75	2727.8	76.4	9052.1	322.9	6390.2	45.5	10035.6	178.6
	14.22	2944.6	179.4	10490.1	518.0	6449.4	158.3	10548.6	372.1
	16.70	2907.6	206.3	11116.5	115.8	6639.2	145.7	10569.2	123.6
	19.17	2918.0	116.7	10706.6	462.5	6591.2	432.2	10636.0	286.8
	78.00	2182.6	98.6	4319.8	226.3	6162.8	455.3	9666.7	746.1
60°	11.75	1931.9	170.0	2653.6	117.8	3543.8	206.0	4463.7	145.1
	14.22	1874.4	110.0	2985.9	134.9	3587.4	186.6	4953.1	252.9
	16.70	2104.6	93.7	3033.7	122.6	3514.5	73.9	5559.9	542.5
	19.17	1774.3	131.6	2965.2	48.8	3722.5	213.2	5834.6	251.8
	78.00	2257.3	88.0	3119.8	98.4	3845.3	149.3	6100.8	168.4
75°	11.75	2849.3	102.3	3900.5	66.0	5297.8	42.4	6998.0	623.4
	14.22	2851.7	62.1	3866.9	150.8	5419.9	200.4	5488.1*	1967.1*
	16.70	2820.5	32.3	3963.8	133.1	5296.7	40.4	3867.8	158.4
	19.17	2809.3	54.4	4017.1	33.6	5394.3	73.2	3799.3	155.5
	78.00	1917.4	107.4	2980.7	183.4	3728.4	82.0	5072.8	161.7

***N = 4, for 75-degree, 14.22 kg, 3.00 m/s impact configuration**

Table 10: Mean Peak Angular Velocity and Standard Deviation for Drop Tower and Full-Surrogate (78.00 kg) in Unhelmeted Impacts

		Velocity (m/s)							
		1.50		2.00		2.50		3.00	
Drop Angle	**Weight (kg)**	**Mean Peak ω**	**Std. Dev.**	**Mean Peak ω**	**Std. Dev.**	**Mean Peak ω**	**Std. Dev.**	**Mean Peak ω**	**Std. Dev.**
30°	11.75	11.8	0.3	14.9	0.8	17.0	0.5	19.6	0.9
	14.22	12.4	0.3	15.7	0.2	17.9	0.8	21.1	0.4
	16.70	12.9	0.4	16.1	0.2	18.0	0.6	22.2	0.4
	19.17	13.5	0.2	16.1	0.3	18.2	0.6	21.0	0.6
	78.00	14.9	0.3	19.0	0.4	21.7	0.5	22.9	1.0
45°	11.75	9.9	0.2	16.3	0.4	10.2	0.3	12.3	0.6
	14.22	9.8	0.3	16.8	1.1	9.8	0.4	13.3	0.4
	16.70	7.6	0.3	17.9	0.3	9.8	0.1	14.0	0.5
	19.17	8.6	2.2	17.8	0.4	9.7	0.6	12.8	0.5
	78.00	5.5	0.5	7.7	1.6	8.5	0.5	11.7	0.9
60°	11.75	9.4	0.2	11.0	0.6	12.2	0.3	15.6	0.2
	14.22	8.1	0.3	10.9	0.3	12.4	0.3	16.8	0.7
	16.70	6.6	0.4	7.8	0.2	9.8	0.5	12.2	0.8
	19.17	7.0	0.3	8.6	0.2	9.3	0.4	11.8	0.3
	78.00	10.4	0.3	12.3	0.2	13.6	0.3	14.9	0.2
75°	11.75	13.4	0.2	15.5	0.6	17.8	0.2	21.5	0.4
	14.22	13.9	0.2	15.1	0.4	17.5	0.2	16.5*	2.7*
	16.70	11.4	0.2	12.5	0.6	13.0	0.1	13.6	0.4
	19.17	9.8	0.1	11.8	0.1	13.4	0.2	14.8	0.2
	78.00	11.0	0.5	13.5	0.1	15.7	0.3	19.6	0.3

***N = 4, for 75-degree, 14.22 kg, 3.00 m/s impact configuration**

To assess the influence of the independent variables, a three-way ANOVA was conducted on the resultant datasets with and without outliers for each of the dependent variables: Peak g, Peak ω, and Peak α. However, Levene's test for equal variances failed with $p < 0.05$ in both ANOVAs, outliers included and removed, indicating that there were unequal variances between levels. Therefore, the three-way ANOVAs were replaced with one-way Welch's ANOVA and Games-Howell post-hoc analysis. The datasets for Peak g, Peak ω, and Peak α were blocked by angle and analyzed using mass as the independent variable. A Shapiro-Wilk test showed that the data was not normally distributed for any of the dependent variables. However, given that the Welch's ANOVA has previously been shown to be fairly robust to normal distribution violations for small sample sizes and that substantial deviations from a normal distribution were not observed in the Q-Q plots, the analysis proceeded as is [83], [84], [85].

Trial 388 (75°, 14.22kg, 3.00 m/s drop tower impact 03) was removed from the data set prior to analysis due to what was deemed a post processing error in the angular velocity calculation as a result of signal noise. Therefore, the data analysis is reported with N = 4 for the 75°, 14.22kg, 3.00 m/s drop tower configuration. All other test configurations are reported with N = 5 as observations of the box plots showed that no outliers were present after the data set was blocked.

Results of the Welch ANOVA indicated that there were statistically significant differences between the full-surrogate and the drop tower for Peak ω ($p<0.05$). For Peak G and Peak α, $p>0.05$ indicates that there are no statistically significant differences for all angles as indicated in *Table 11*.

Table 11: Robust Tests of Equality of Means for Welch ANOVA, P<0.05 indicates significant differences.

Angle	Measure	Statistic	df1	df2	P
30°	Peak_g	0.240	4	47.395	0.914
	Peak_ω	**3.853**	**4**	**47.440**	**0.009**
	Peak_α	0.247	4	47.383	0.910
45°	Peak_g	0.036	4	47.480	0.997
	Peak_ω	**8.523**	**4**	**47.078**	**<0.001**
	Peak_α	1.841	4	47.434	0.137
60°	Peak_g	0.113	4	47.461	0.977
	Peak_ω	**15.240**	**4**	**47.047**	**<0.001**
	Peak_α	0.855	4	47.160	0.498
75°	Peak_g	0.203	4	46.936	0.935
	Peak_ω	**19.937**	**4**	**43.701**	**<0.001**
	Peak_α	2.467	4	46.361	0.058

Results of the Games-Howell post hoc tests for Peak ω at each angle are summarized in Table 12. Post hoc tests were not performed for Peak g or Peak α as they were not found to significantly differ between all drop tower masses and the full-surrogate. The observed significant differences in Peak ω between the full-surrogate and each of the drop tower weights revealed a dependency on the test angle. At 30°, the lowest drop tower mass of 11.75kg significantly differed from the full-surrogate, while at 60° and 75° the higher drop tower masses of 16.70kg and 19.17kg differ significantly. All drop tower configurations significantly differed from the full-surrogate at 45°. Table 13 shows how the drop tower under- or over- estimates the peak kinematics of the full-surrogate.

Table 12: multiple comparisons for Peak ω from Games-Howell post-hoc test for full-surrogate (78.00kg) and drop tower masses at each unhelmeted impact angle.

Multiple Comparisons								
							95% Confidence Interval	
Angle	Dependent Variable			Mean Difference (I-J)	Std. Error	Sig.	Lower Bound	Upper Bound
30°	Peak_ω	78 kg	**11.75 kg**	**3.8***	**1.0**	**0.003**	**1.006**	**6.604**
			14.22 kg	2.9	1.0	0.057	-0.1	5.8
			16.70 kg	2.3	1.1	0.197	-0.7	5.4
			19.17 kg	2.4	1.0	0.105	-0.3	5.2
45°	Peak_ω	78 kg	**11.75 kg**	**-3.8***	**0.8**	**<0.001**	**-6.1**	**-1.5**
			14.22 kg	**-4.1***	**0.9**	**<0.001**	**-6.6**	**-1.5**
			16.70 kg	**-4.0***	**1.1**	**0.006**	**-7.0**	**-0.9**
			19.17 kg	**-3.8***	**1.0**	**0.005**	**-6.8**	**-0.9**
60°	Peak_ω	78 kg	11.75 kg	0.7	0.7	0.792	-1.1	2.6
			14.22 kg	0.7	0.8	0.891	-1.6	3.1
			16.70 kg	**3.7***	**0.6**	**<0.001**	**1.9**	**5.5**
			19.17 kg	**3.7***	**0.6**	**<0.001**	**2.1**	**5.2**
75°	Peak_ω	78 kg	11.75 kg	-2.1	1.0	0.241	-5.0	0.8
			14.22 kg	-0.7	0.8	0.900	-3.2	1.7
			16.70 kg	**2.3***	**0.8**	**0.040**	**0.1**	**4.6**
			19.17 kg	**2.5***	**0.8**	**0.043**	**0.1**	**5.0**

* The mean difference is significant at the 0.05 level. **Bold** font indicates configurations where the drop tower was found to significantly differ from full-body impacts.

Table 13: Summary of Differences in Kinematic Measures Between a Full-Surrogate and Weighted Drop Tower in Unhelmeted Impacts at Tested Angles and Velocities.

		30°				45°				60°				75°			
Full-Surrogate	Carriage Weight	11.75 kg	14.22 kg	16.70 kg	19.17 kg	11.75 kg	14.22 kg	16.70 kg	19.17 kg	11.75 kg	14.22 kg	16.70 kg	19.17 kg	11.75 kg	14.22 kg	16.70 kg	19.17 kg
	Peak g																
	Peak α																
	Peak ω	X				X	X	X	X			X	X			X	X

Blue indicates that the drop tower underestimates peak kinematics, red indicates that the drop tower overestimates peak kinematics, and X through the cell denotes statistically significant difference.

Ensemble average time traces between the full-surrogate and the four tested drop tower masses are shown in (Figure 14 – Figure 17) for resultant angular velocity at each angle and test velocity. At 45°, it was found that the angular velocity statistically differed from the full-surrogate for each of the four carriage masses tested, Figure 14. Upon examining the time trace comparisons, the significant difference appears to be limited to the lower velocity testing. Specifically at 2.00 m/s (Figure 14-B), the resultant Peak ω of the drop tower, across all tested weights, was found to be between 71.5% and 79.8% greater than the resultant Peak ω of the full-surrogate. This significant difference is attributed to testing at a cross over point between no-slip and slip conditions between the headform and the impact surface. When testing at 45°. At 2.50 and 3.00 m/s (Figure 14-C,D) the drop tower provided an acceptable representation of the full-surrogate as the headform only slips on the impact surface at these greater velocities.

In 30° 60° and 75° configurations, the 11.75kg and 14.22kg drop tower configurations were found to not significantly differ from the Peak ω of the surrogate for at least one of the tested carriage masses. However, Representative ensemble average time traces (Figure 18 – Figure 19) of the angular velocity Y Component for the drop tower and full-surrogate, for 60° and 75° impacts, show that the drop tower Peak ω occurs in the opposite direction and at a later time instance during impact. These difference in direction and time instance are identified in Figure 18 while the causes of these differences are discussed in detail in Chapter 5.

A

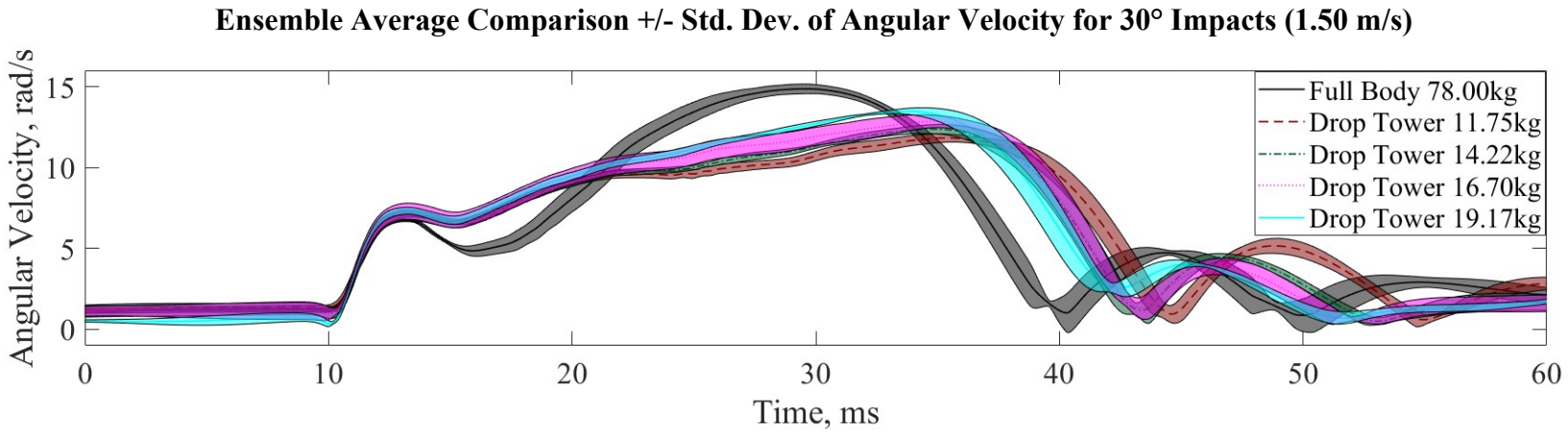
Ensemble Average Comparison +/- Std. Dev. of Angular Velocity for 30° Impacts (1.50 m/s)
Angular Velocity, rad/s
Time, ms
Full Body 78.00kg
Drop Tower 11.75kg
Drop Tower 14.22kg
Drop Tower 16.70kg
Drop Tower 19.17kg

B

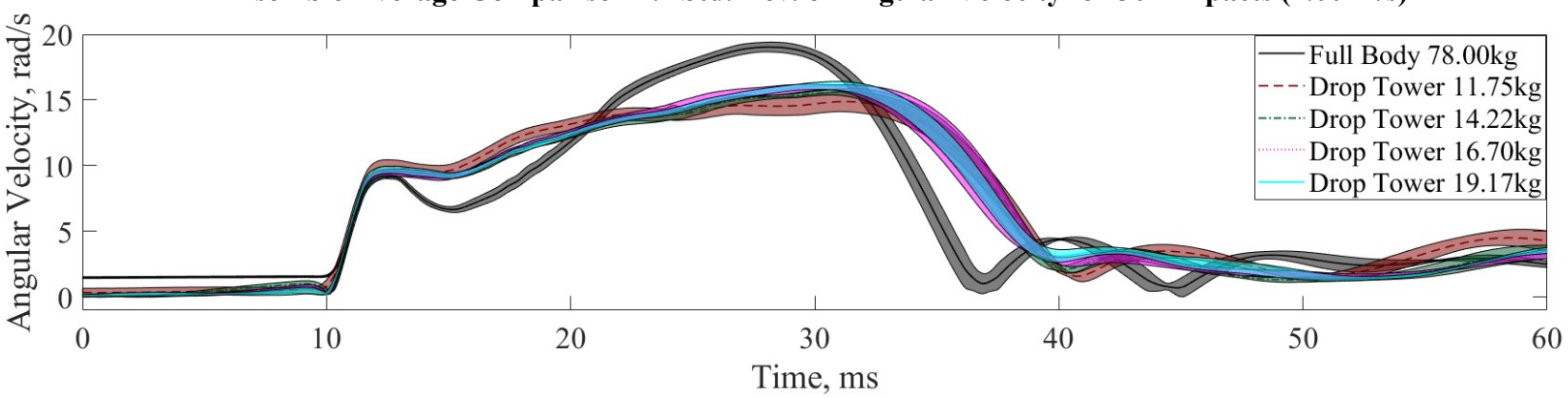
Ensemble Average Comparison +/- Std. Dev. of Angular Velocity for 30° Impacts (2.00 m/s)
Angular Velocity, rad/s
Time, ms
Full Body 78.00kg
Drop Tower 11.75kg
Drop Tower 14.22kg
Drop Tower 16.70kg
Drop Tower 19.17kg

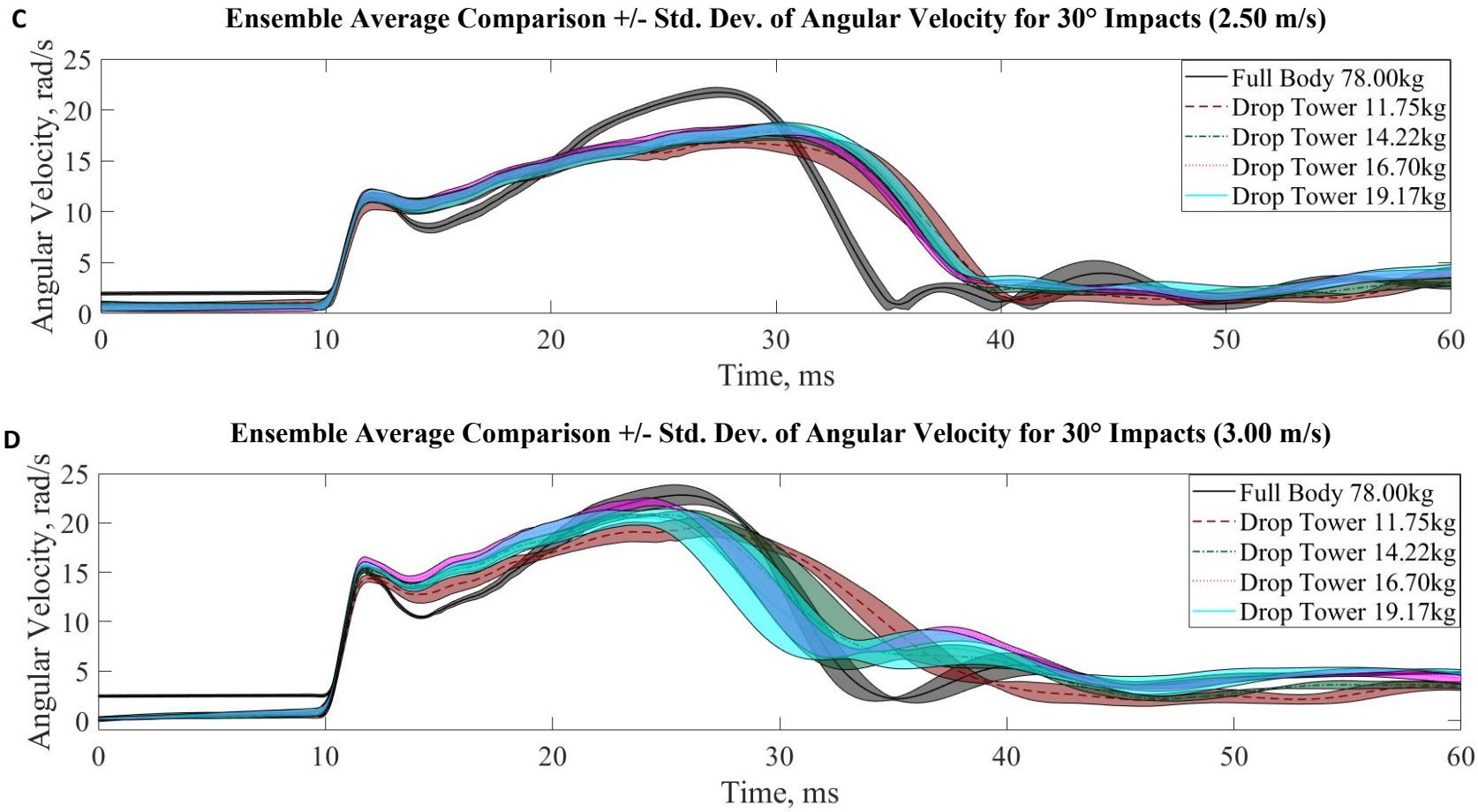

Figure 14: Time trace comparisons of angular velocity over time for each drop carriage mass and full-surrogate in 30° impacts at each unhelmeted test velocity. A) 1.50m/s, B)2.00m/s, C) 2.50m/s, D) 3.00m/s.

A

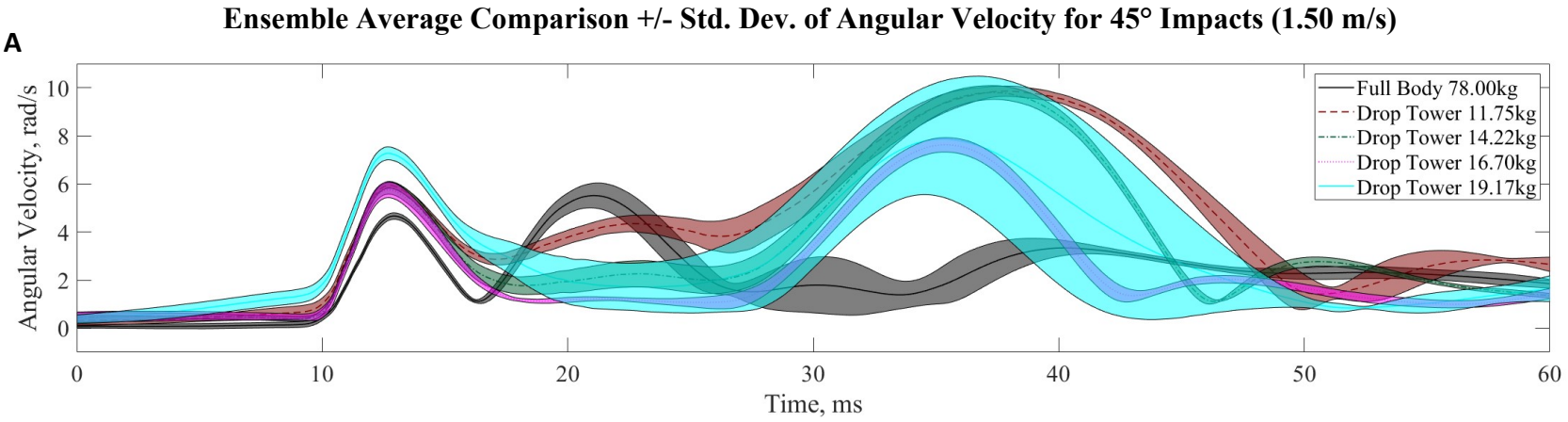
Ensemble Average Comparison +/- Std. Dev. of Angular Velocity for 45° Impacts (1.50 m/s)
Angular Velocity, rad/s
Time, ms
Full Body 78.00kg
Drop Tower 11.75kg
Drop Tower 14.22kg
Drop Tower 16.70kg
Drop Tower 19.17kg

B

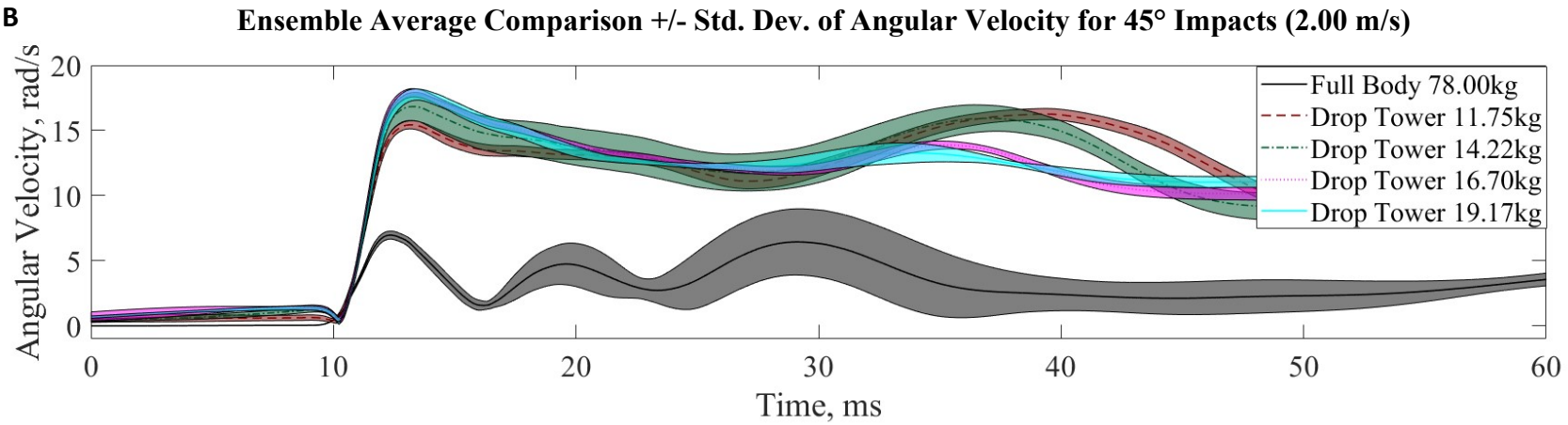
Ensemble Average Comparison +/- Std. Dev. of Angular Velocity for 45° Impacts (2.00 m/s)
Angular Velocity, rad/s
Time, ms
Full Body 78.00kg
Drop Tower 11.75kg
Drop Tower 14.22kg
Drop Tower 16.70kg
Drop Tower 19.17kg

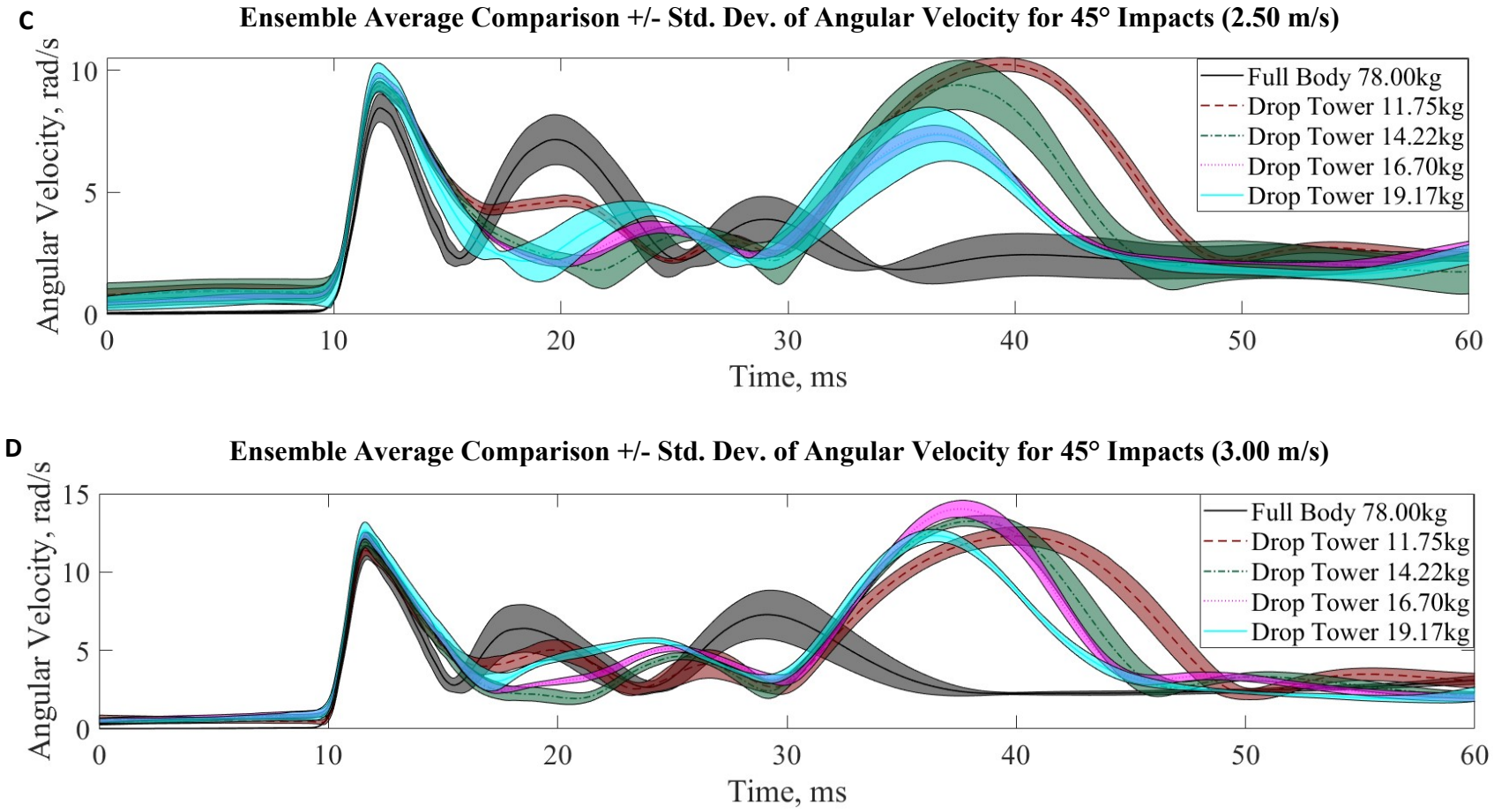

Figure 15: Time trace comparisons of angular velocity over time for each drop carriage mass and full-surrogate in 45° impacts at each unhelmeted test velocity. A) 1.50m/s, B)2.00m/s, C) 2.50m/s, D) 3.00m/s.

A

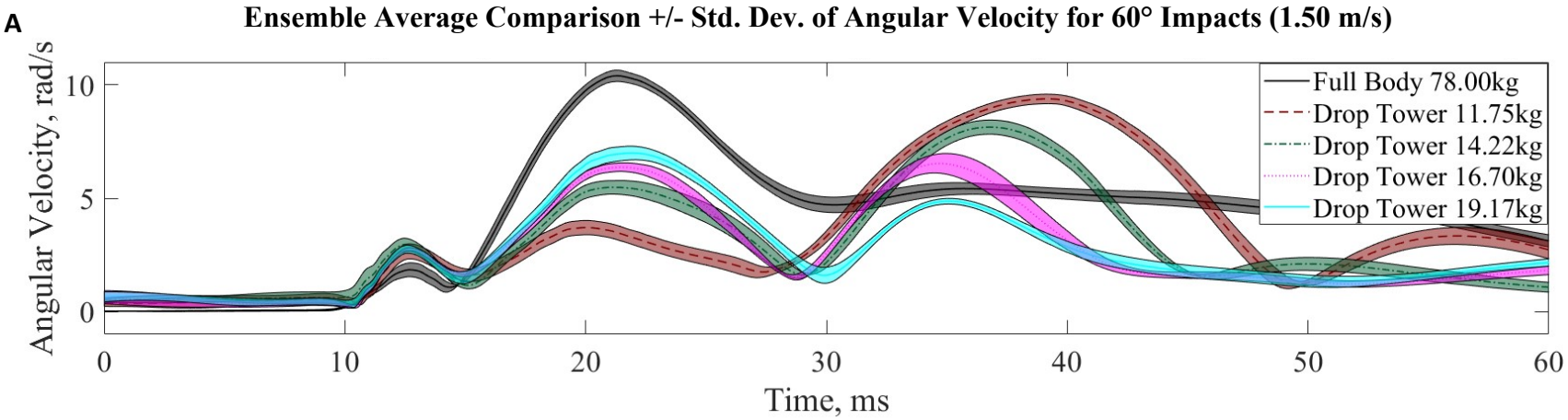
Ensemble Average Comparison +/- Std. Dev. of Angular Velocity for 60° Impacts (1.50 m/s)
Angular Velocity, rad/s
Time, ms
Full Body 78.00kg
Drop Tower 11.75kg
Drop Tower 14.22kg
Drop Tower 16.70kg
Drop Tower 19.17kg

B

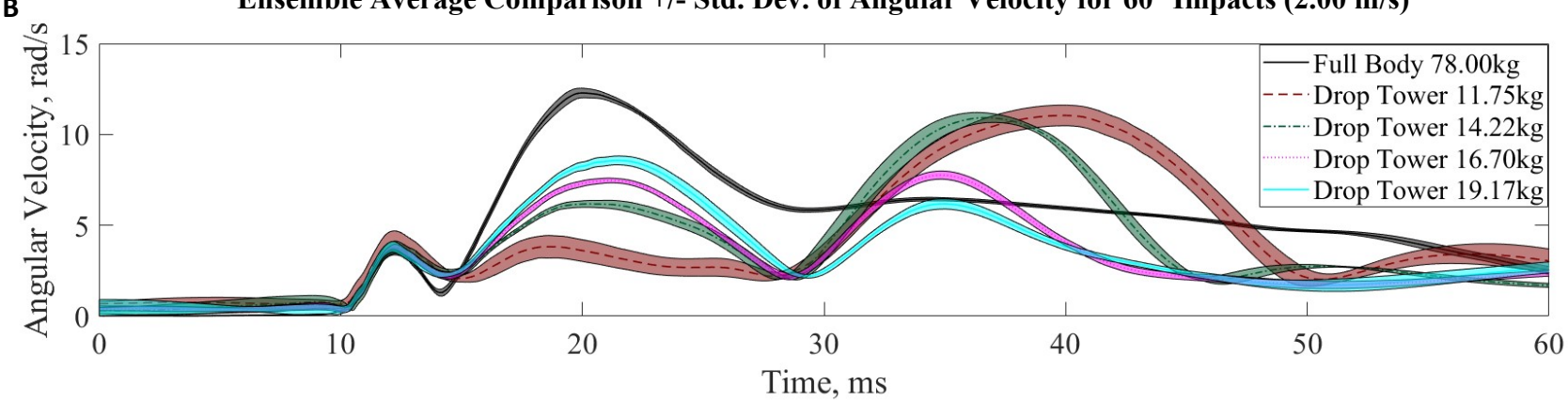
Ensemble Average Comparison +/- Std. Dev. of Angular Velocity for 60° Impacts (2.00 m/s)
Angular Velocity, rad/s
Time, ms
Full Body 78.00kg
Drop Tower 11.75kg
Drop Tower 14.22kg
Drop Tower 16.70kg
Drop Tower 19.17kg

C

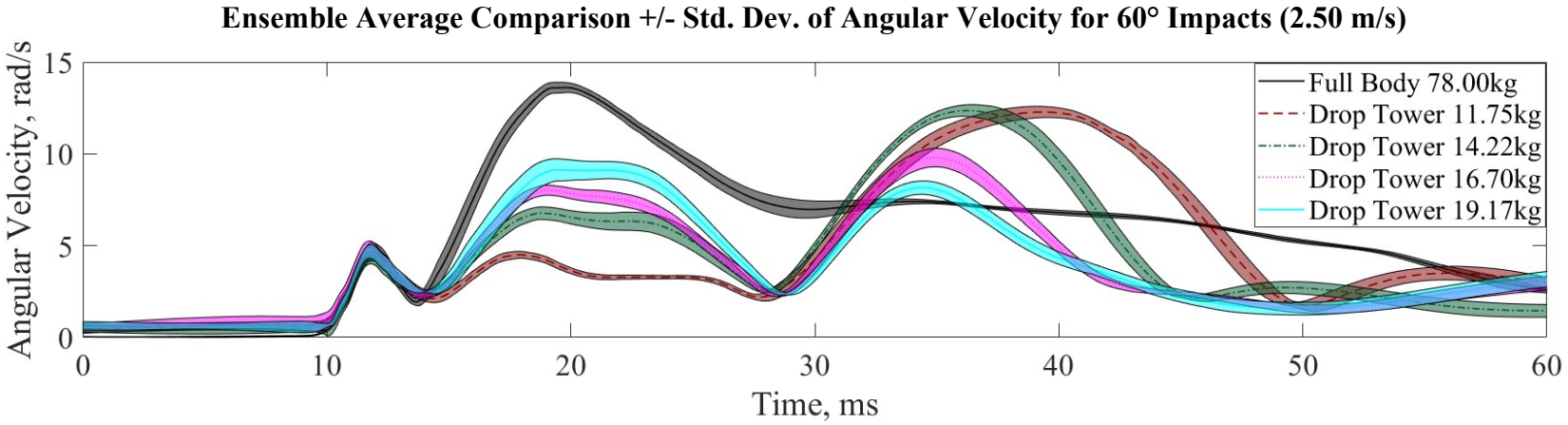

D

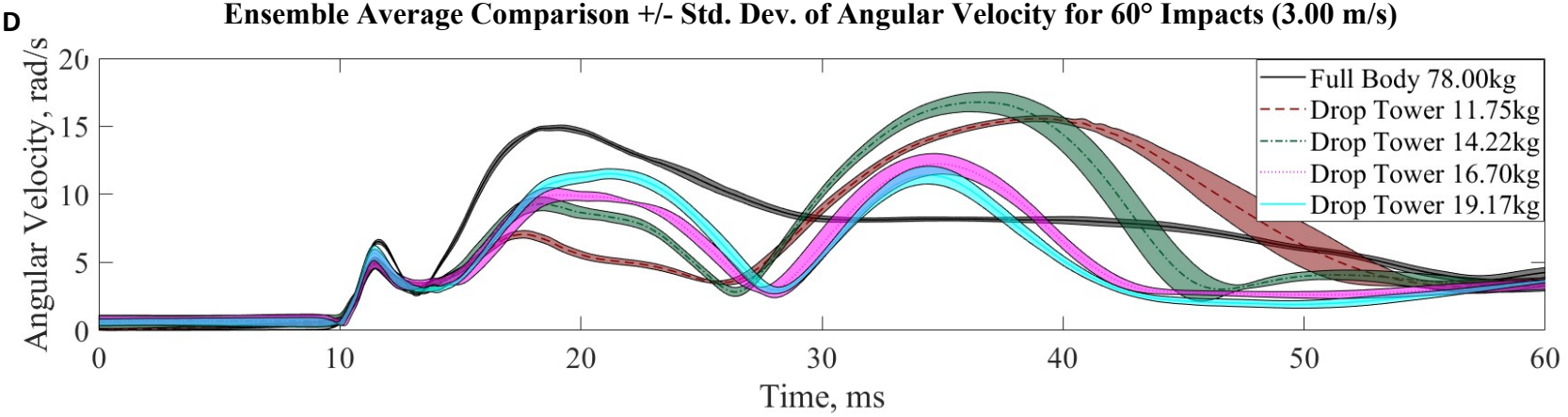

Figure 16: Time trace comparisons of angular velocity over time for each drop carriage mass and full-surrogate in 60° impacts at each unhelmeted test velocity. A) 1.50m/s, B)2.00m/s, C) 2.50m/s, D) 3.00m/s. ensemble

A

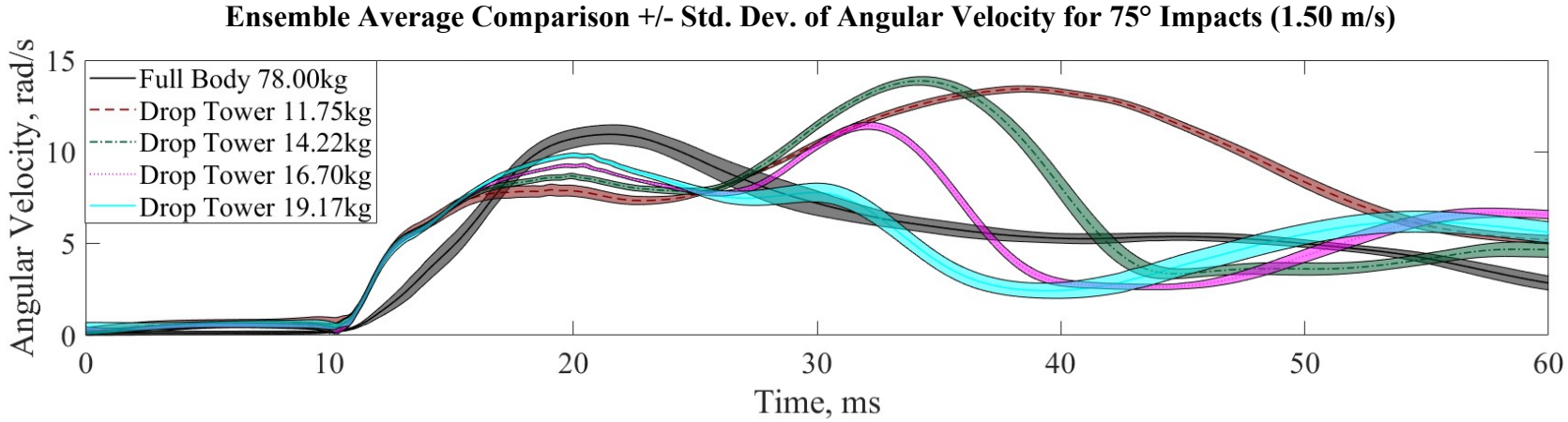
Ensemble Average Comparison +/- Std. Dev. of Angular Velocity for 75° Impacts (1.50 m/s)
Full Body 78.00kg
Drop Tower 11.75kg
Drop Tower 14.22kg
Drop Tower 16.70kg
Drop Tower 19.17kg
Angular Velocity, rad/s
Time, ms
0
5
10
15
0
10
20
30
40
50
60

B

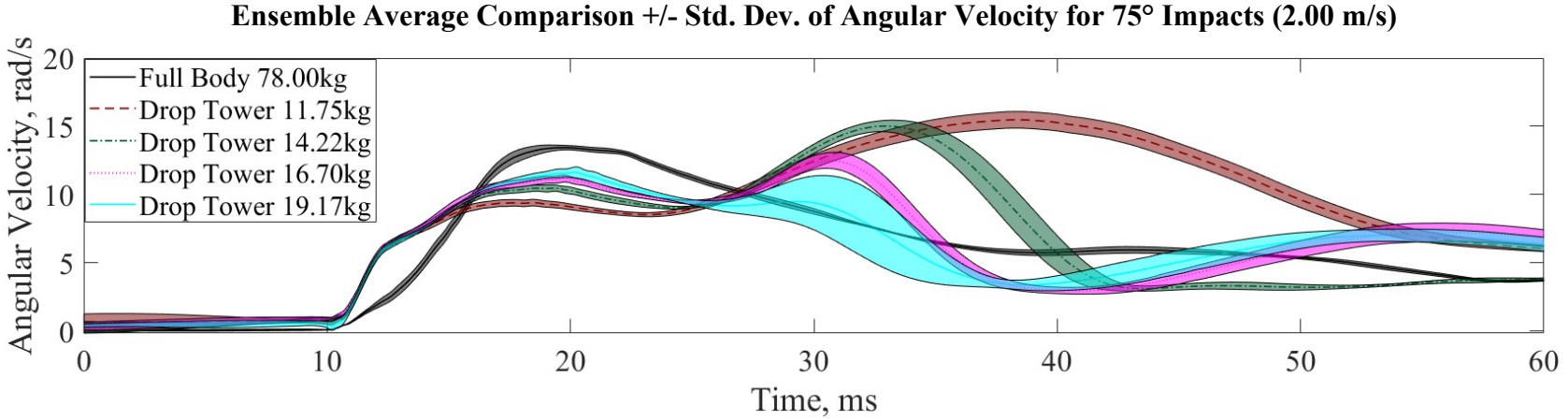
Ensemble Average Comparison +/- Std. Dev. of Angular Velocity for 75° Impacts (2.00 m/s)
Full Body 78.00kg
Drop Tower 11.75kg
Drop Tower 14.22kg
Drop Tower 16.70kg
Drop Tower 19.17kg
Angular Velocity, rad/s
Time, ms
0
5
10
15
20
0
10
20
30
40
50
60

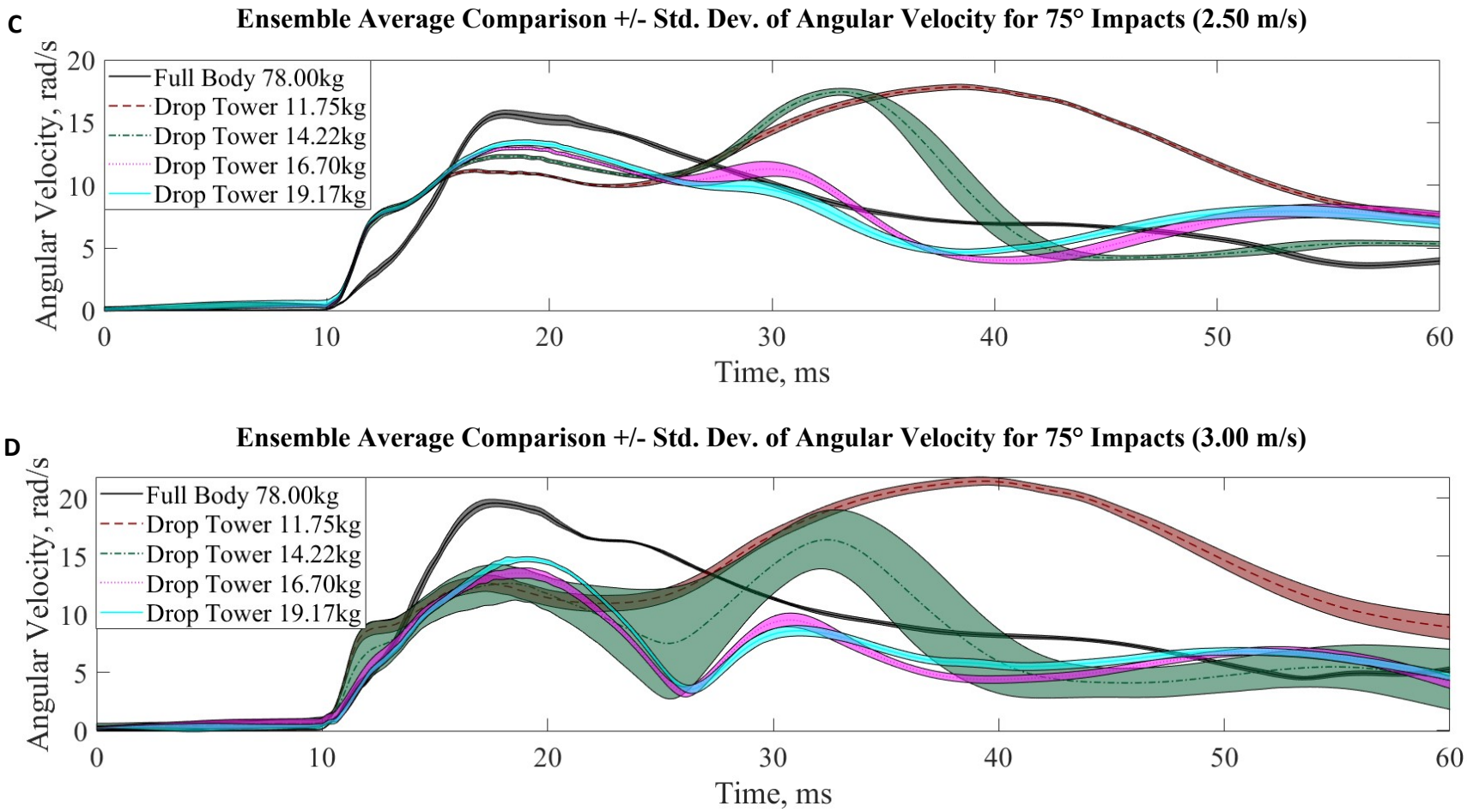

Figure 17: Time trace comparisons of angular velocity over time for each drop carriage mass and full-surrogate in 75° impacts at each unhelmeted test velocity. A) 1.50m/s, B)2.00m/s, C) 2.50m/s, D) 3.00m/s

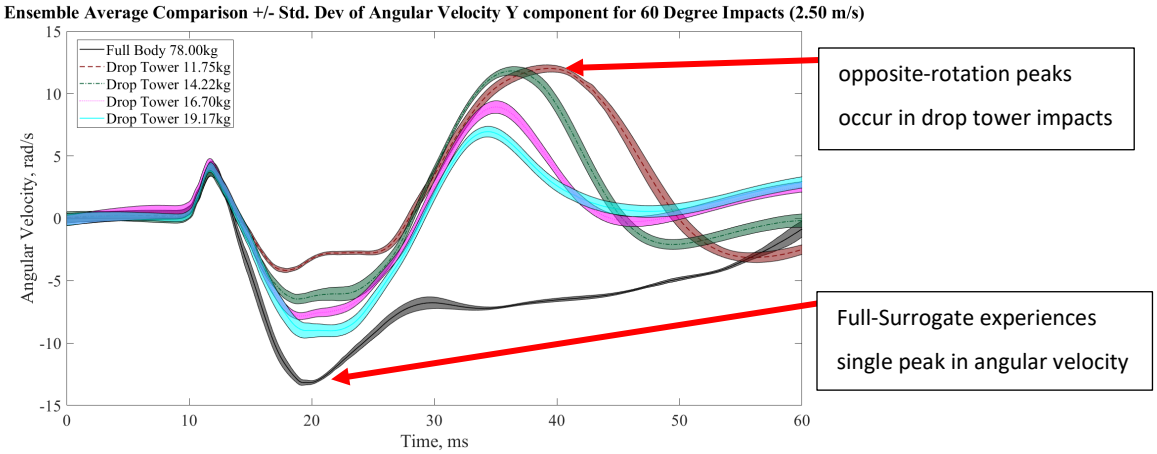

Figure 18: Ensemble time trace of Y component angular velocity, shown for 2.50m/s, 60° unhelmeted impact. Angular velocity peak for drop tower impacts occur in opposite direction and at a later time instance after initial impact compared to full-surrogate impacts

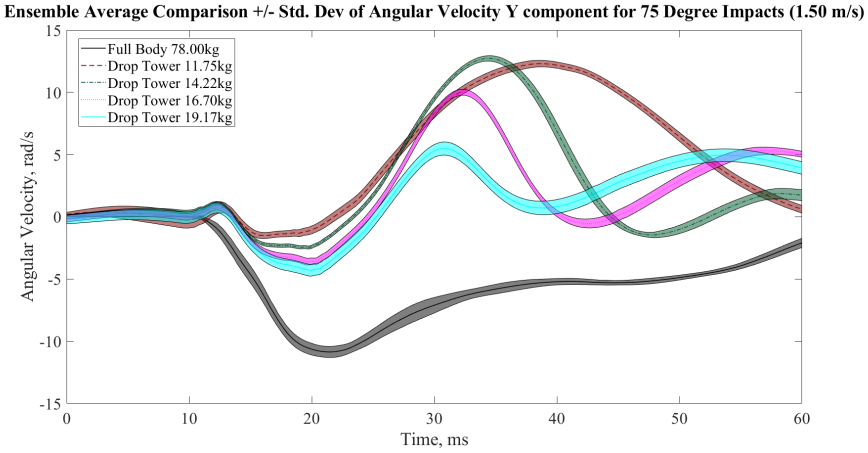

Figure 19:Ensemble time trace of Y component angular velocity, shown for 1.50m/s, 75° unhelmeted impact. Angular velocity peak for drop tower impacts occur in opposite direction and at a later time instance after initial impact compared to full-surrogate impacts.

4.2 Helmeted Impact Results

A summary of the mean impact angle and associated SDs are reported in Table 7 for each helmeted impact configuration of the full-body and drop tower experiments. Means for Peak g, Peak ω, and Peak α are summarized for each impact angle and reported in Table *14* – Table *16*. Head kinematics are reported as the peak resultant value of the X, Y, and Z components.

Table 14: Mean Peak Linear Acceleration and Standard Deviation for Drop Tower and Full-Surrogate Helmeted Impacts

		Low Velocity (3.00 m/s)		**High Velocity (4.50 m/s)**	
Angle	**Weight (kg)**	**Mean Peak g**	**Std. Dev. Peak g**	**Mean Peak g**	**Std. Dev. Peak g**
30°	Drop Tower (11.75)	65.1	2.2	83.4	1.8
	Drop Tower (19.17)	65.2	3.5	87.7	2.2
	Full-Surrogate (78.00)	77.6	6.3	133.3	6.6
75°	Drop Tower (11.7)	66.0	2.3	86.2	6.4
	Drop Tower (19.2)	65.2	2.3	90.1	9.6
	Full-Surrogate (78.00)	48.7	4.2	85.8	6.0

Table 15: Mean Peak Angular Velocity and Standard Deviation for Drop Tower and Full-Surrogate Helmeted Impacts

		Low Velocity (3.00 m/s)		**High Velocity (4.50 m/s)**	
Angle	**Weight (kg)**	**Mean Peak ω**	**Std. Dev. Peak ω**	**Mean Peak ω**	**Std. Dev. Peak ω**
30°	Drop Tower (11.75)	22.6	0.3	26.4	0.8
	Drop Tower (19.17)	29.6	2.6	37.1	1.3
	Full-Body (78.00)	26.9	0.4	39.9	0.3
75°	Drop Tower (11.7)	16.3	1.0	22.5	1.9
	Drop Tower (19.2)	16.9	1.1	23.5	0.5
	Full-Surrogate (78.00)	13.2	1.5	22.2	0.6

Table 16: Mean Peak Angular Acceleration and Standard Deviation for Drop Tower and Full-Surrogate Helmeted Impacts

		Low Velocity (3.00 m/s)		High Velocity (4.50 m/s)	
Angle	**Weight (kg)**	**Mean Peak α**	**Std. Dev. Peak α**	**Mean Peak α**	**Std. Dev. Peak α**
30°	Drop Tower (11.75)	2460.9	21.0	3068.0	240.2
	Drop Tower (19.17)	3531.5	200.6	8409.2	1079.7
	Full-Surrogate (78.00)	3540.8	345.1	6443.2	835.7
75°	Drop Tower (11.75)	3283.4	533.7	4290.0	244.9
	Drop Tower (19.17)	4645.5	1624.7	7536.4	452.7
	Full-Surrogate (78.00)	4179.4	138.8	6155.0	1068.9

A three-way ANOVA was conducted on the resultant datasets for Peak g, Peak ω, and Peak α to assess the influence of the independent variables. No outliers were detected in the dataset, therefore no secondary analyses to test outlier effects were required. Similar to the unhelmeted test series, Levene's test for equal variances failed, $p < 0.05$, indicating that there were unequal variances between levels. The three-way ANOVAs were replaced with one-way ANOVAs and post-hoc analysis by blocking the datasets by angle and impact velocity and using mass as the independent variable. Shapiro-Wilks tests of the one-way ANOVAs showed that the data was normally distributed, $p > 0.05$, for each of the dependent variables except for the following configurations:

- Peak ω of the 19.2 kg 30° high-speed drop tower impact series.
- Peak G of the full-surrogate 75° low-speed impact series
- Peak α of the full-surrogate 75° low-speed impact series

However, for the same reasons described in the unhelmeted test series, the analysis proceeded.

A Levene's test for equal variances of each of the configurations indicated that the dependent variables in the following configurations yielded $p<0.05$ and, therefore, were evaluated using a one-way Welch ANOVA along with Games-Howell post-hoc analysis.

- Peak ω of the 30° low-speed impact series
- Peak α of the 75° low-speed impact series
- Peak ω of the 75° high-speed impact series

The dependent variables for all other configurations were evaluated using a standard one-way ANOVA and Tukey test post-hoc analysis.

The results of the standard one-way ANOVAs are summarized in Table 17 and the results of the Welch's ANOVAs, for the cases with unequal variances, are shown in Table *18.* Results of the Tukey Test, when significant differences were found in the one-way ANOVAs, are shown in Table *19*, while results of the Games-Howell test, when significant differences were found in Welch's ANOVA, are shown in Table 20.

Table 17 One-Way ANOVA Results for Test Configurations with Equal Variances as Evaluated by Levene's Test for Equal Variances.

Angle	Velocity (m/s)	Measure	Sum of Squares	df	Mean Square	F	Sig.
30°	3.00	**Peak g**	**309.9**	**2**	**154.9**	**8.191**	**0.019**
		Peak α	**2312531.0**	**2**	**1156265.5**	**21.705**	**0.002**
	4.50	**Peak g**	**4588.4**	**2**	**2294.1**	**132.232**	**0.000**
		Peak α	**43787034.4**	**2**	**21893517.2**	**34.179**	**0.001**
		Peak ω	**302.2**	**2**	**151.1**	**187.853**	**0.000**
75°	3.00	**Peak g**	**569.2**	**2**	**284.6**	**30.419**	**0.001**
		Peak ω	**23.2**	**2**	**11.5**	**7.585**	**0.023**
	4.50	Peak g	33.7	2	16.8	0.299	0.752
		Peak α	**15925562.9**	**2**	**7962781.4**	**16.973**	**0.003**
BOLD indicates significant differences found, $p<0.05$							

Table 18: Robust Tests of Equality of Means for Welch's ANOVA, P<0.05 Indicates Significant Differences.

Angle	Velocity (m/s)	Measure	Statistic	df1	df2	P
30°	**3.00**	**Peak ω**	**93.916**	**2**	**3.427**	**0.001**
75°	3.00	Peak α	3.335	2	2.853	0.179
	4.50	Peak ω	3.547	2	3.590	0.141
BOLD indicates significant differences found, p<0.05						

Table 19: Multiple Comparisons from Tukey Post-hoc Test for Full-Surrogate (78.00 kg) and Drop Tower Masses for Helmeted Impact Configurations.

Multiple Comparisons (Tukey Test)									
Angle	**Velocity (m/s)**	**Dependent Variable**			**Mean Difference (I-J)**	**Std. Error**	**Sig.**	**95% Confidence Interval**	
								Lower Bound	**Upper Bound**
30°	3.00	Peak g	78 kg	**11.75 kg**	**12.5***	**3.6**	**0.029**	**1.6**	**23.4**
				19.17 kg	**12.4***	**3.6**	**0.030**	**1.5**	**23.3**
		Peak α	78 kg	**11.75 kg**	**1079.9***	**188.5**	**0.003**	**501.7**	**1658.1**
				19.17 kg	9.2	188.5	0.999	-569.0	587.4
	4.50	Peak g	78 kg	**11.75 kg**	**49.9***	**3.4**	**0.000**	**39.4**	**60.3**
				19.17 kg	**45.6***	**3.4**	**0.000**	**35.2**	**56.1**
		Peak α	78 kg	**11.75 kg**	**3375.2***	**653.5**	**0.005**	**1370.2**	**5380.3**
				19.17 kg	-1966.0	653.5	0.054	-3971.1	39.0
		Peak ω	78 kg	**11.75 kg**	**13.5***	**0.5**	**0.000**	**11.2**	**15.7**
				19.17 kg	2.8	0.8	0.105	-1.2	6.8
75°	3.00	Peak g	78 kg	**11.75 kg**	**-17.3***	**2.5**	**0.001**	**-24.9**	**-9.6**
				19.17 kg	**-16.4***	**2.5**	**0.001**	**-24.1**	**-8.9**
		Peak ω	78 kg	11.75 kg	-3.1	1.0	0.051	-6.2	0.0
				19.17 kg	**-3.7***	**1.0**	**0.026**	**-6.8**	**-0.6**
	4.50	Peak α	78 kg	**11.75 kg**	**1865.0***	**559.2**	**0.036**	**149.1**	**3581.0**
				19.17 kg	-1381.4	559.2	0.106	-3097.3	334.6
* The mean difference is significant at the 0.05 level. **Bold** indicates configurations where the drop tower was found to significantly differ from full-surrogate impacts.									

Table 20: Multiple comparisons from Games-Howell post-hoc test for full-surrogate (78.00kg) and drop tower masses.

Multiple Comparisons (Games-Howell)									
Angle	**Velocity (m/s)**	**Dependent Variable**			**Mean Difference (I-J)**	**Std. Error**	**Sig.**	**95% Confidence Interval**	
								Lower Bound	**Upper Bound**
30°	3.00	Peak ω	78 kg	**11.75 kg**	**13.5***	**0.5**	**0.000**	**11.2**	**15.7**
				19.17 kg	2.8	0.8	0.105	-1.2	6.8
* The mean difference is significant at the 0.05 level. **Bold** indicates configurations where the drop tower was found to significantly differ from full-surrogate impacts.									

These results are summarized in Table 21 and show that at least one of the kinematic measures of interest significantly differ between the drop tower and the full-surrogate, except for the 75° 4.50m/s configuration where the 19.17 kg drop tower was found to not significantly differ.

Table 21: Summary of Differences in Kinematic Measures Between a Full-Surrogate and Weighted Drop Tower at Tested Angles and Velocities.

		30 deg				75 deg			
		3.00 m/s		4.50 m/s		3.00 m/s		4.50 m/s	
Full-Surrogate	Carriage Weight	11.75kg	19.17kg	11.75kg	19.17kg	11.75kg	19.17kg	11.75kg	19.17kg
	Peak g	X	X	X	X	X	X		
	Peak α	X		X				X	
	Peak ω	X		X			X		
Blue indicates that the drop tower underestimates peak kinematics, red indicates that the drop tower overestimates peak kinematics, and X through the cell denotes statistically significant difference.									

The causes of the differences in kinematic responses at different angles and how changing carriage mass influences the kinematic response are detailed in the Chapter 5 discussion for helmeted impacts.

Comparative time traces between the full-surrogate and the two drop tower configurations for each test level are shown in (Figure 20 – Figure 21) for Peak g, Peak ω and Peak α. Observing the Peak ω plot for the 75° 4.50m/s configuration indicates that although the Peak ω does not significantly differ between the 19.17 kg drop tower and the full-surrogate, the drop tower peak occurs later in the impact. This alludes to the same delayed, opposite rotation resulting from carriage rebound observed in the unhelmeted impact.

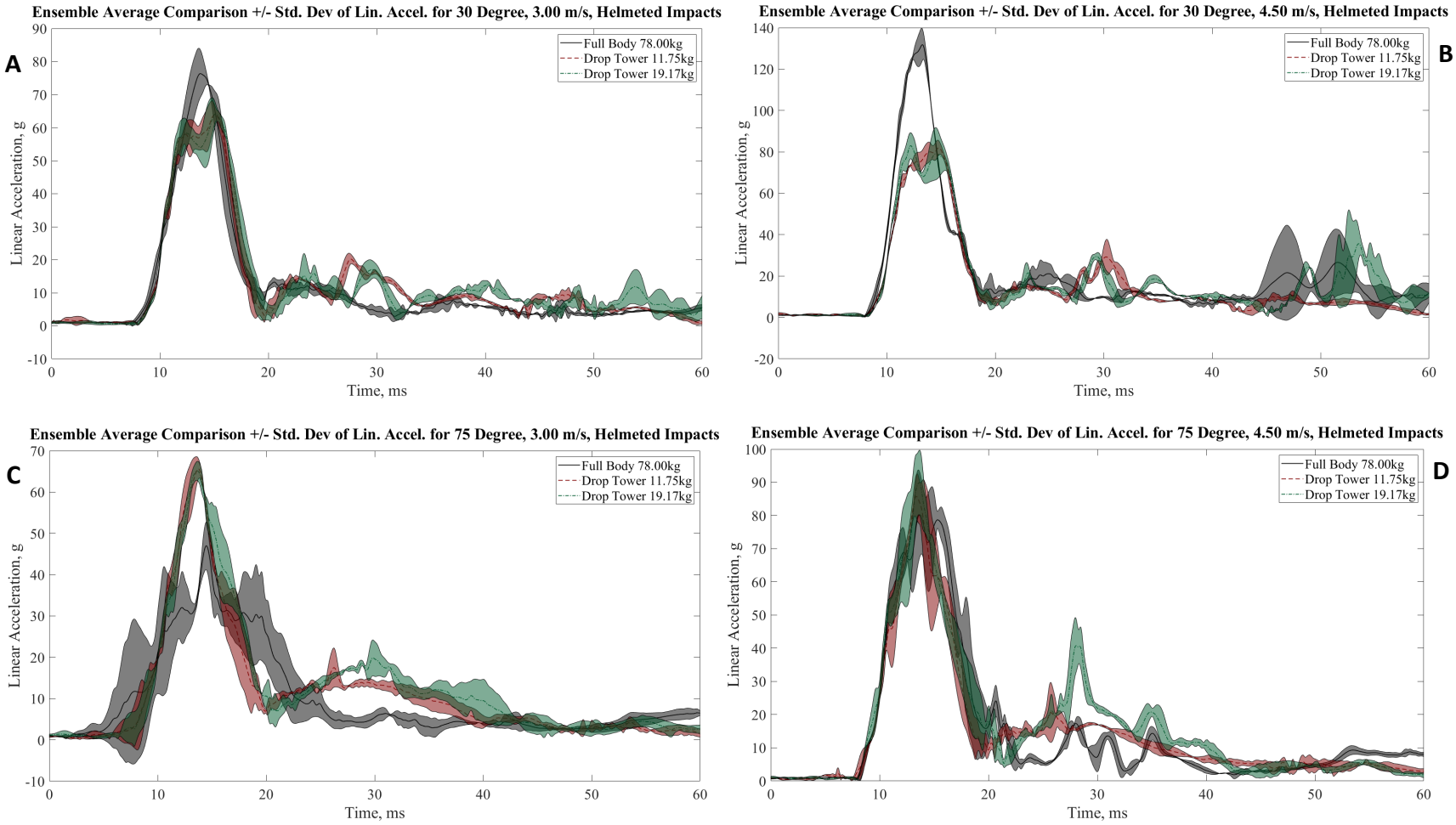

Figure 20:Ensemble time trace comparisons between 11.75kg drop tower, 19.17kg drop tower, and full-surrogate linear acceleration for helmeted impact scenarios. A) 30°, 3.00 m/s B) 30°, 4.50 m/s C) 75°, 3.00 m/s D) 75°, 4.50 m/s

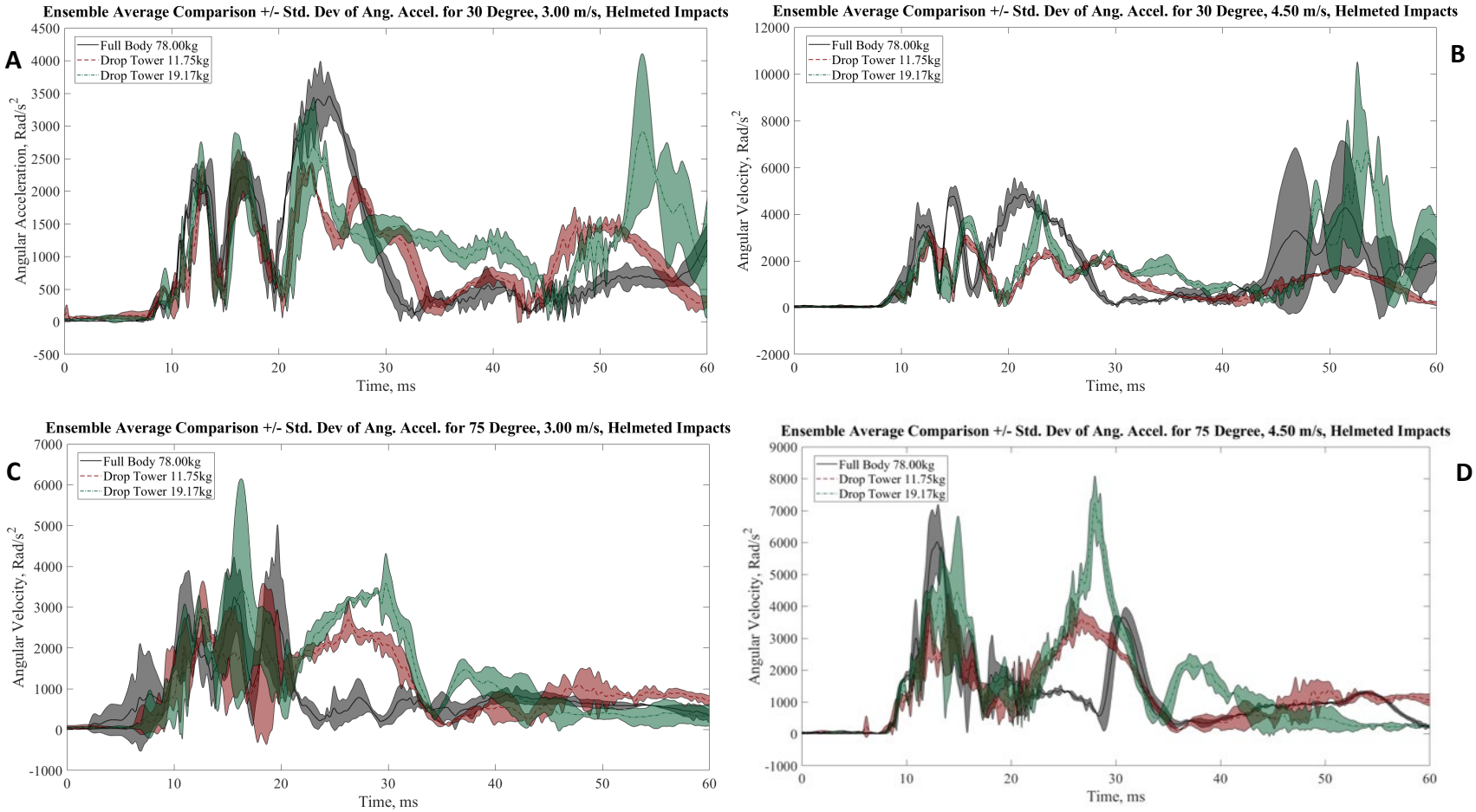

Figure 21:Ensemble time trace comparisons between 11.75kg drop tower, 19.17kg drop tower, and full-surrogate angular acceleration for helmeted impact scenarios. A) 30°, 3.00 m/s B) 30°, 4.50 m/s C) 75°, 3.00 m/s D) 75°, 4.50 m/s

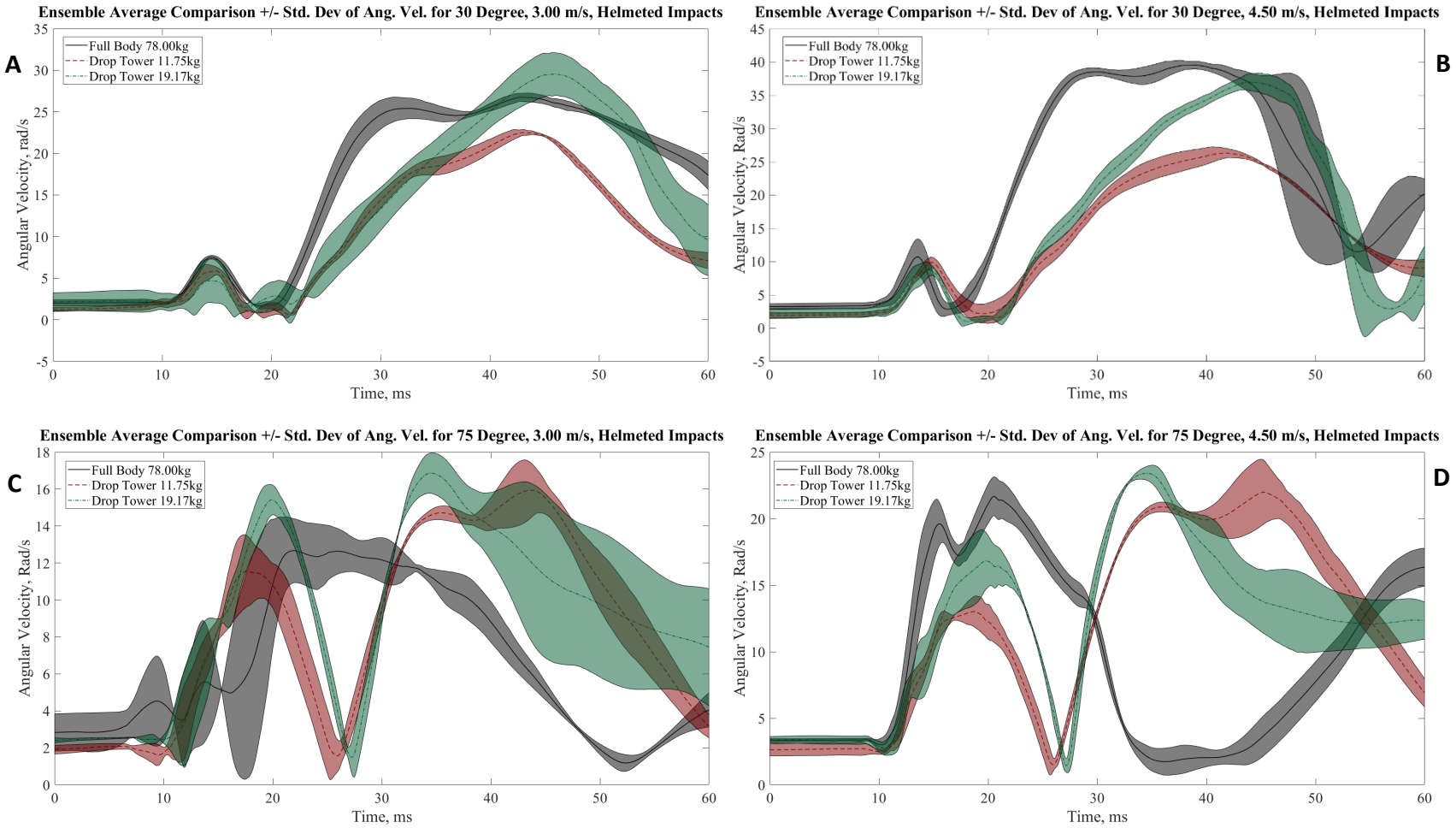

Figure 22:Ensemble time trace comparisons between 11.75kg drop tower, 19.17kg drop tower, and full-surrogate angular velocity for helmeted impact scenarios. A) 30°, 3.00 m/s B) 30°, 4.50 m/s C) 75°, 3.00 m/s D) 75°, 4.50 m/s

Looking at the Y component of Peak ω, of the 75° tests confirms that the drop tower experiences the same delayed opposite rotation of the head that was found in the unhelmeted impacts. The drop tower constraints that cause this opposite rotation are discussed in Chapter 5.

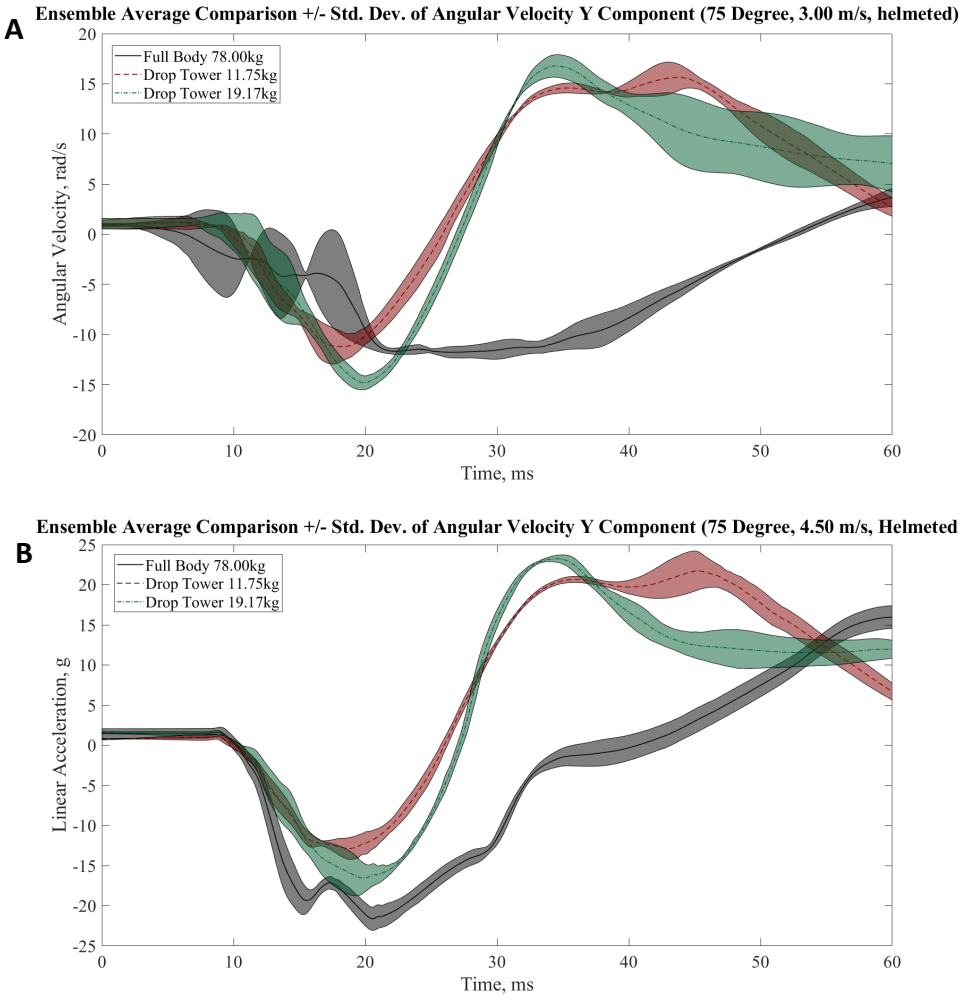

Figure 23: Y Component time trace comparison of angular velocity for 75° helmeted impacts show delayed peaks in opposite direction for drop tower impacts compared to full-surrogate. A) 3.00m/s B) 4.50m/s.

5.0 Discussion

This chapter summarizes the results of the helmeted and unhelmeted impact series and discusses the modified drop experiment's ability to replicate a falling surrogate in the tested impact orientations.

5.1 Unhelmeted Impacts

5.1.1 Comparison of drop tower and full-surrogate in unhelmeted impact

The unhelmeted impact comparisons between a guided drop tower system, which enables both linear and rotational motion, and a free-falling surrogate showed that a drop tower produces Peak g and Peak α that are not statistically different from the full-surrogate. As such, the drop tower provides an acceptable representation of these measures in unhelmeted scenarios up to 3.0m/s. However, differences were found between the drop tower and the full-surrogate when comparing Peak ω, which varied across the tested impact angles. For 30° impacts the full-surrogate and drop tower had peak kinematics that didn't significantly differ, with the exception of the 11.22kg configuration, and the direction of Peak ω was consistent. This means that at 30° the drop tower can be said to be capable of achieving peak kinematics that are representative of an unhelmeted fall, for the range of test velocities studied, provided the assembly has sufficient mass. These equivalent kinematics differ from what was observed across the other test angles as 45°, 60°, and 75° yielded either different peak angular kinematics or delayed opposite rotation. Specifically at 45°, Peak ω differed significantly at 1.50 and 2.00 m/s which is attributed to differences in motion of the head between the two scenarios after impact. High speed video of the drop tower and the full-surrogate impacts at 2.00 m/s showed that the head slips on the impact surface in both the drop tower and full-surrogate impacts (Figure 24). Due to the constraints of the drop tower, the head is unable to translate along the impact surface when this slip occurs and as a result, the head only rotates. This is unlike the unconstrained full-surrogate, which primarily translates along the impact surface when this slip occurs which yields a lower Peak ω than the drop tower.

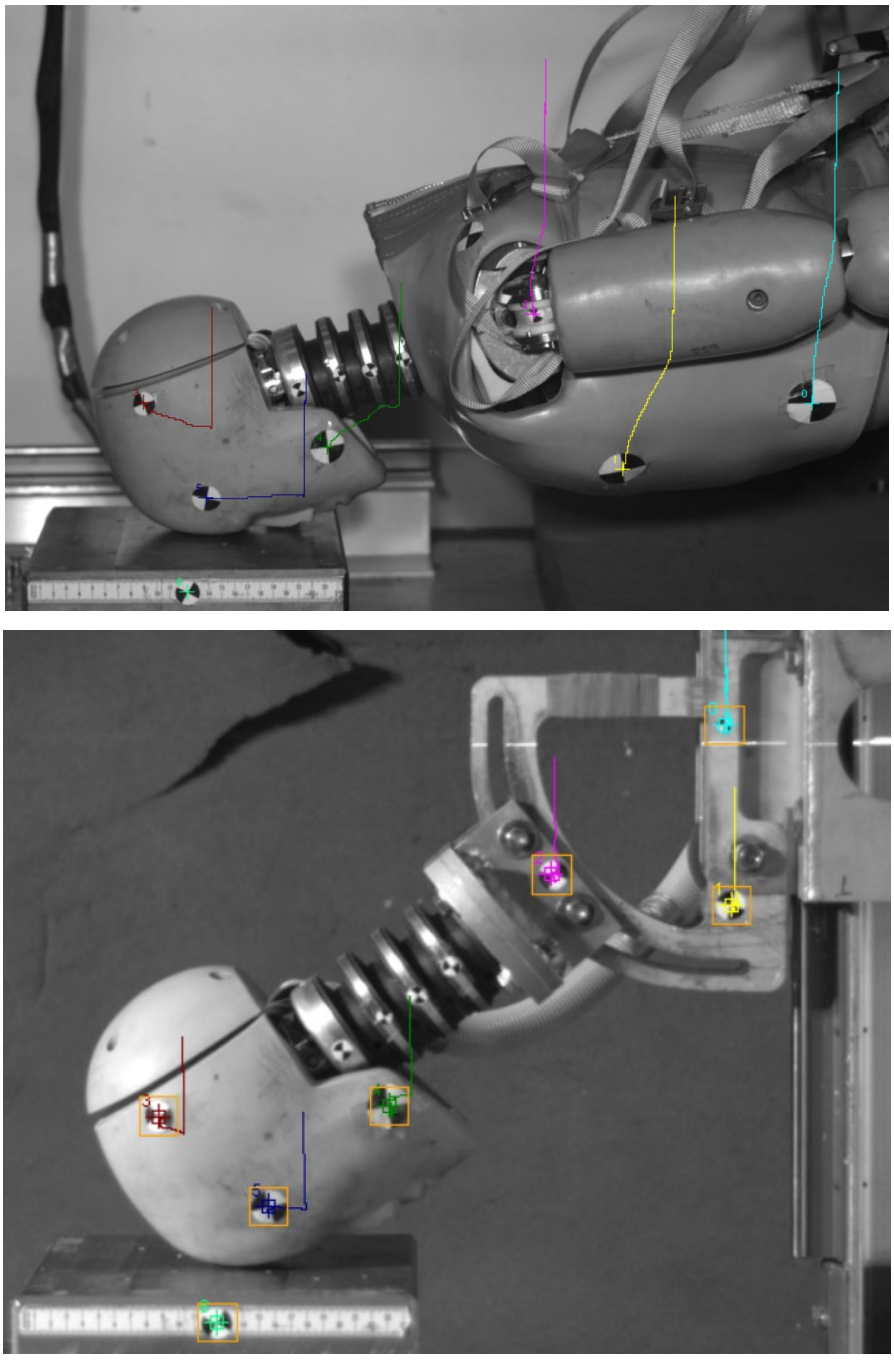

Figure 24: Head motion comparison in unhelmeted impact at 2.00 m/s and 45° neck angle showing translation of head along impact surface in free-falling surrogate (top) and head rotation in 11.75kg drop tower (bottom). Coloured trace lines indicate motion path of tracking targets just prior to and immediately after impact.

Although this difference in motion was not exclusive to the 45° 2.00 m/s impacts it was the most significant difference in Peak ω observed across all test configurations. An additional observation is that the surrogate body's ability to rotate freely reduces the amount of neck extension that occurs relative to what is seen in the drop tower impacts. As the objective of this work was to identify a single drop carriage mass that can be used irrespective of impact velocity for a given angle, the significant differences in Peak ω at 1.50 m/s and 2.00 m/s means that the drop tower cannot be said to be representative of a 45° fall.

At 60° and 75° the 11.75kg and 14.22kg drop tower configurations also displayed the differences in motion that were observed in the 45° configuration. These differences between the drop tower and full-surrogate are likely attributable to the same single degree of freedom constraint of the drop tower carriage assembly that produced the significant differences in Peak ω at 45°. This constraint in motion only allows for head rotation and motion in a single axis, which is unlike the free fall impact that can translate and rotate about all axes. This difference in motion of the head is evident in high-speed video tracking of head position during and immediately after impact in the 60° and 75° configurations. Further, high-speed video from low drop carriage mass impacts at these angles show that the initial head/neck rotation after impact occurs in the same direction as the full-surrogate but after the initial impact the drop carriage rebounds, which produces the delayed opposite rotation that was found in the component time trace data. Representative video traces for these differences in motion are shown for 75°, 2.50 m/s impacts in (Figure 25).

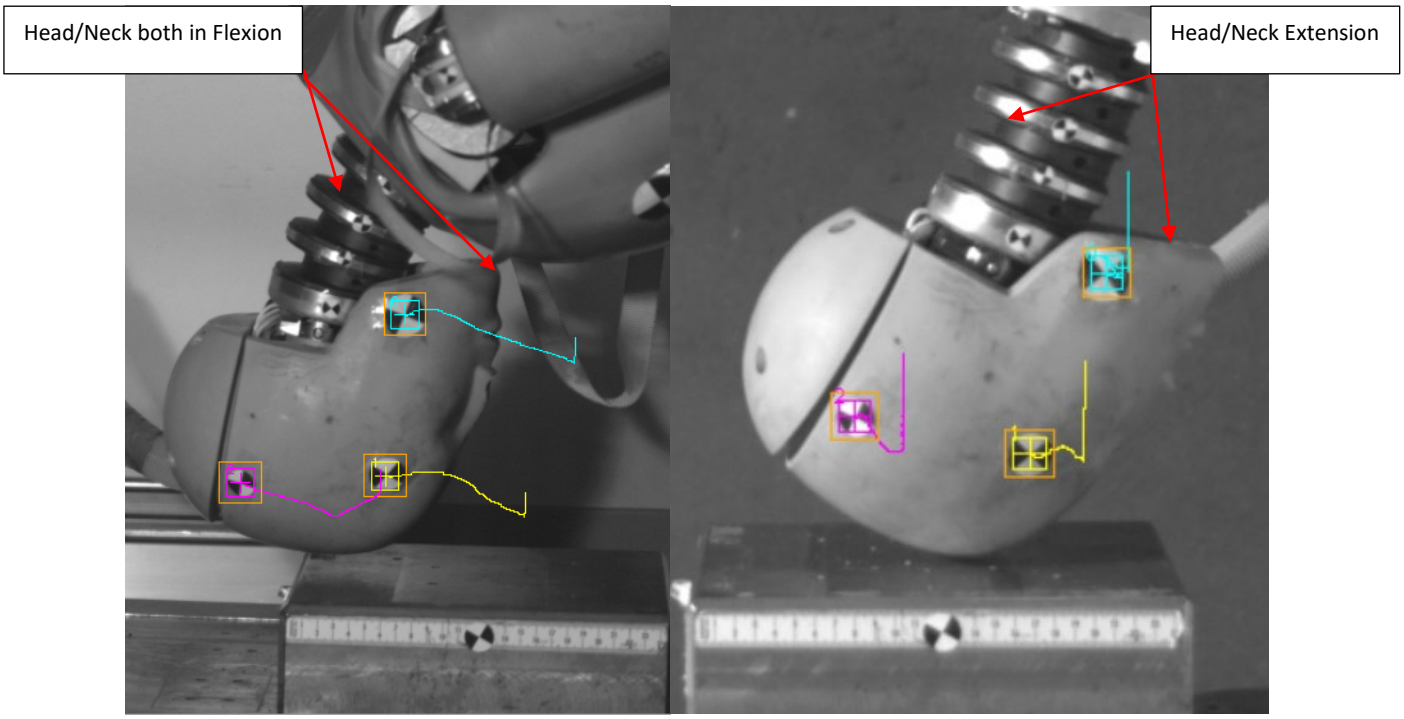

Figure 25: Head motion comparison of free-falling surrogate (left) and 11.75kg drop tower (right) in unhelmeted impact at 2.5m/s and 75° neck angle depicting head/neck flexion in full-surrogate impacts and head/neck extension in low mass drop tower impacts after rebound.

Observation of 30° high-speed film shows that the drop tower assemblies and the full-surrogate yield head and neck motion in the same directions (Figure 26), which is in agreement with resultant and component time traces reported in Chapter 4.

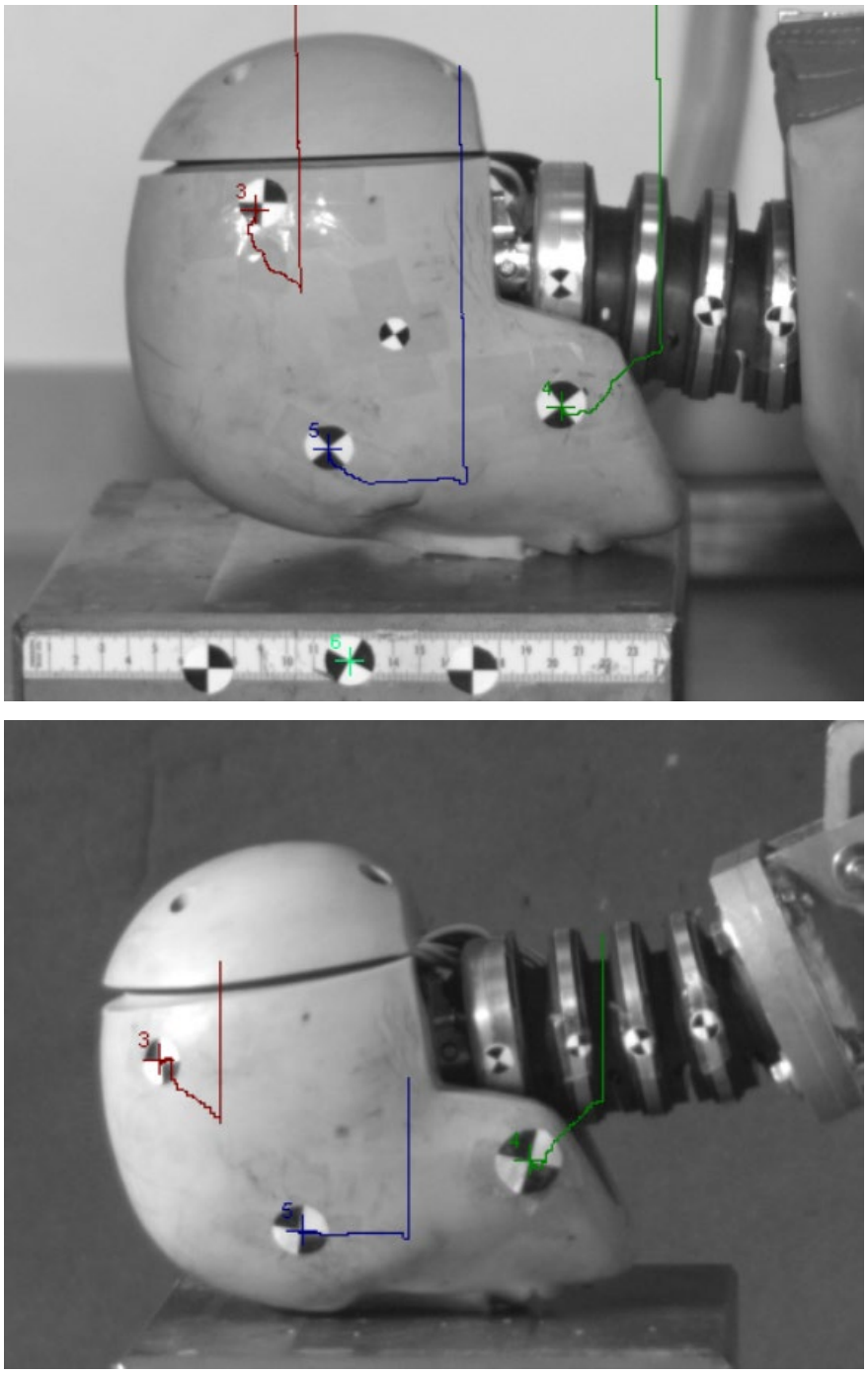

Figure 26: Head motion comparison in unhelmeted impact at 2.5m/s and 30° neck angle show similar head motion, despite different neck curvature, after impact between free-falling surrogate (top) and drop tower (bottom)

5.1.2 Summary of Unhelmeted Impact Comparison

The comparison between the kinematic responses of the guided drop tower and the full-surrogate in unhelmeted frontal falls yielded the following key findings:

- the drop tower provides an acceptable approximation of the linear acceleration likely to be experienced by a falling person in a headfirst frontal impact up to 3.00 m/s.
- the drop tower generally yields angular kinematics that significantly differ from the full-surrogate.
- An exception to the significantly different angular kinematics was observed for the high mass 30° drop tower configurations (14.22kg – 19.17kg) which provided an acceptable approximation of both linear and angular kinematics of the full-surrogate.
- In steep angle impacts, 60° and 75°, a drop tower yields resultant angular velocities that are a product of kinematic components that occur in the opposite direction and are delayed due to rebound of the drop tower carriage.

These key findings from the unhelmeted impacts determined that the guided drop tower is a suitable device for evaluating the linear response of a head in fall injury research within the tested parameters of this study. However, when studying the angular response, which is a primary contributor to mTBI of the head, the drop tower did not provide an acceptable approximation of a person falling with exception to a 30° impact angle provided sufficient carriage mass is used. These differences in angular velocity are due to the lack of degrees of freedom available with the guided drop tower as compared to a full-surrogate which has no constraints to its degrees of freedom. These constraints result in a Peak ω that differs in either magnitude or direction and time instance. As such further advancements are necessary before using a drop tower to evaluate the injury risk associated with resultant angular kinematics. These findings are not withstanding the drop tower's potential influence on helmet liner performance, which is discussed in the following section.

5.2 Helmeted Impacts

5.1.2 Comparison of Drop Tower and Full-Surrogate in Helmeted Impact

The helmeted impact series was conducted to determine if the inclusion of a helmet in headfirst impacts would yield an equivalent kinematic response between the drop tower and the falling surrogate at current helmet standard test velocities as well as at a higher velocity that is closer to average low height fall velocities. The drop tower was found to significantly differ from the full-surrogate at the current helmet standard velocity for both carriage weights and impact angles. The 11.75kg test at 30° was found to significantly underestimate Peak g, Peak α and Peak ω at both test velocities, while the 19.17kg configuration was found to significantly underestimate Peak g only. These findings indicate that in shallow angle impacts, 30°, at the current standard test velocity of 3.0m/s, a drop tower fitted with a Hybrid III head/neck is likely to underestimate the Peak g that would be experienced in a low height fall by 21.73% ± 4.37% and 23.02% ± 7.65% with an 11.75kg and 19.17 kg carriage, respectively. At 4.50 m/s, the drop tower further underestimated the full-surrogate with the difference in resultant Peak g increasing to 59.54% ± 5.02% and 51.36% ± 3.44% for the 11.75kg and 19.17 kg carriage, respectively.

The cause for underestimations of Peak g in helmeted free-falling headform impacts were reviewed in Chapter 3 where it was found that a reduction in helmet liner compression, relative to the compression that was observed in full-surrogate falls, was attributable to the reduction in Peak g [77]. Although helmet liner compression was not measured in this study, it is likely that a difference in helmet liner compression also exists between the guided drop tower and the full-surrogate. This is primarily evidenced by Peak g not significantly differing between the drop tower and the full-surrogate in unhelmeted impacts along with the findings of Hering et al. [77]. When also considering the angular kinematics that are enabled by the Hybrid III head/neck alone, a drop tower experiment can provide resultant peak angular responses similar to a full-surrogate, provided that (1) a sufficient carriage mass is used and (2) the underestimation of Peak g is corrected. However, the same phenomenon of delayed and opposite signed peak component angular velocities observed in the unhelmeted case was also observed in the helmeted case. This indicates that the method in which the peak resultant measures are achieved differ.

At 75° the two carriage masses were both found to overestimate Peak g at 3.00m/s by 30.05% ± 3.03% and 28.87% ± 3.48% for the 11.75kg and 19.17 kg carriage respectively. At 4.50m/s, both drop tower configurations yielded similar Peak g to the full-surrogate. This suggests that for steep angle impacts the weighted drop tower provides a similar response to that of a full-surrogate at 4.50 m/s, which is more representative of a fall from height when considering Peak g alone. However, at the current standard test velocity of 3.00m/s a drop tower equipped with a Hybrid III head/neck underestimates a helmet's impact attenuation capability, which means personnel falling at those velocities would experience a less severe impact. This difference in linear response compared to shallow angle impacts is likely due to how the mass of the carriage and body act through the Hybrid III neck. The mass of the carriage and the body act more directly through the axis of the neck in steep angle impacts and are likely producing similar neck compression within the time duration of the initial impact. This would subsequently produce helmet liner compression comparable to that seen in full-surrogate tests, which is unlike the difference in liner performance that was observed in shallow angle impacts where the carriage and body mass do not primarily act through the neck axis. When also considering angular kinematics, the only drop tower configuration found to not significantly differ from the full-surrogate was the 19.75 kg carriage at 75° and 4.50 m/s. However, as previously noted in the unhelmeted series, Peak ω of this configuration occurs later and in the opposite direction of the full-surrogate.

5.2.2 Summary of Helmeted Impact Comparison

Comparisons between the drop tower equipped with a Hybrid III head/neck and a full-surrogate in helmeted impacts at current test standard impact velocities and a velocity that more closely represents low height falls yielded the following critical findings:

- Generally, the drop tower was not found to closely replicate the angular kinematics in either magnitude, direction, or time instance.
- The drop tower significantly underestimates the Peak g that is likely to be experienced in shallow angle headfirst frontal impacts but overestimates Peak g in steep angle impacts regardless of carriage mass.

There are two main factors that were identified as the primary causes of differing kinematic responses in the tested scenarios. First, the constraints imparted by the drop tower's guide rail limits motion to a single axis which prevents translation along the impact surface and second, the rebound of the drop carriage assembly immediately after initial impact creates separation between the Hybrid head/neck and the impact surface which leads to opposite rotation of the head/neck. Second, there are dissimilarities in how the guided drop tower and the full-surrogate engage the helmet liner which causes differences between the resulting kinematic response. This result is consistent with what has been previously reported on in the comparison between isolated headforms and full-surrogates [77]. These findings indicate that, in its current form, a guided drop tower equipped with a Hybrid III head/neck does not provide an equivalent impact to a helmeted, headfirst, low height fall and such an impact may not be achieved using additional carriage mass alone.

5.3 Research Limitations

While the Hybrid III surrogate provides a representative model of a person in a fall from height, it is not without limitations. First, the model used in this experimental work was a standard Hybrid III 50th male model, which is primarily intended to conform to a car seat for use in frontal car crash testing [58], [59]. To conform with car seats, the dummy has a molded pelvis that holds it in a seated position which needed to be pulled into a standing position via a backstrap. This strap effectively added a tensioning member along the surrogate's body which may have altered the response of the dummy body to the impacts. As no body kinematics were measured, this alteration to the body was not of significant concern; however, it is possible that this may have had some effect on how the body influences head kinematics. A second consideration is that the Hybrid III model itself is designed with repeatability and manufacturing in mind, which means it does not provide an exact replication of a human response to impact. For example, the response of the neck has previously been shown to be too stiff when compared to a human neck in direct impact scenarios [59], [86]. This means that the kinematic differences between a drop tower and an actual fall from height may differ even more than what was found in this study if compared to actual fall data or if repeated with a more compliant neck surrogate intended for direct impact [60].

Another limitation of this work was the setup and repeatability of the full-surrogate impacts. Although every effort was taken to ensure that each impact was setup identically, there was still a possibility for variance. Alignment of each impact was checked using laser levels and positioning targets which were subject to human interpretation when checking alignment. The rigging equipment also had to be reset between each impact, which required small length adjustments of the straps to set the fall angle; this was also subject to interpretation of the analog angle finder placed on the neck. Finally, for the full-surrogate impacts, the impact angle was measured from high-speed video using the best interpretation possible of the neckline; however, this method of measurement is subject to some potential errors in measurement, such as what was deemed to be the correct points along the neckline, potential curvature of the neck during free fall, and spatial quantization error of the selected point.

For the drop tower impacts, the limitations and possible sources of error surrounding setup and repeatability were limited compared to the full-surrogate, as an electromagnetic release mechanism was fixed in place prior to conducting each set of impacts which eliminated the variability in fall height and orientation. However, the magnetic release may have had an influence on fall velocity between impacts as it has a small amount of residual holding strength once it is switched off, which could introduce a small amount of resistance on the drop carriage when released. The way this residual holding strength influenced the carriage would likely vary between each impact. This potential effect couldn't be quantified due to the spatial quantization error of the high-speed camera limiting the ability to make precise velocity measurements.

Finally, in the helmeted impact series, the helmet liner compression could not be directly measured during impact testing. Due to this, the conclusion on the differences in Peak g being a result of differing liner compression, between a free-falling surrogate and a guided drop tower, are speculative based on previously reported findings [77] and the results of the unhelmeted series where linear acceleration differences didn't occur.

5.4 Recommendations for Future Work

A key finding of this work was that kinematic differences between a guided drop tower and a full-surrogate are primarily attributable to the limitations that a guided drop tower imposes on post-impact head motion relative to the unconstrained full-surrogate. This restriction should be investigated in future work through changes to the design of the drop carriage to enable more degrees of freedom such as a detachable head, neck, and ballast that can be released from the rail at impact.

Equipment limitations resulted in an inability to achieve a high enough velocity to be fully representative of an average low height fall; if achieved, this may produce greater differences between the surrogate and the drop tower. Conversely, in helmeted impacts the differences in helmet liner performance may be overcome through full compression of the helmet liner. Understanding these potential differences at more representative velocities would further contribute to the knowledge of how standards should be developed to represent a low height fall.

This study also only focused on frontal impacts to the head/helmet and did not consider other possible impact locations, such as the side, back, or oblique. Continued efforts toward developing a better understanding of how a drop tower compares to a falling person and the standards that can be implemented should consider these impact locations as they are likely to yield a different response from the frontal impacts. However, it is also worth noting the limitations in the design of the Hybrid III neck. As mentioned previously, the Hybrid III was originally intended for frontal car crash testing and not direct impact [59], [86]. In particular, the construction of the Occipital-Condyle joint of the Hybrid III is not conducive to side impact and is unlikely to yield a highly biofidelic response [10]. As such, consideration should also be given to the use of a more biofidelic neck that is intended for omnidirectional, direct impact if investigating other impact locations [60].

6.0 Conclusion

This chapter provides a summary of this works motivation and key findings as well as outlines its contributions.

6.1 Summary

Military personnel experience high rates of fall related mTBI despite the use of protective headgear that is intended to provide protection from head in a fall from height. The development of new helmet technology and testing methods is imperative to reducing the threat of fall induced head injury. The objectives of the work presented in this thesis were to develop an understanding of how the kinematic response of a drop tower, the current method for testing helmets, differs from the kinematic response of a person falling from height and if alterations to carriage mass can achieve a more representative response. Of primary focus was the inclusion of rotational kinematics, which is currently omitted from current pass-fail test criterion despite being a primary contributor to mTBI, in addition to the commonly measured linear kinematics. The results of this work showed that the guided drop tower is limited in its ability to provide a representative fall from height due to its constraint on the number of degrees of freedom relative to a person falling. Further, helmet liner compression in a fall from height is believed to differ between the drop tower and a falling surrogate, which yields a difference in the kinematic response of the two systems which can result in an overestimation of the protection provided by a helmet during a fall. Finally it was found that these differences aren't universally offset across the tested configurations by changing the drop carriage mass. This suggests that the guided drop tower requires further advancements, beyond the addition of carriage mass, if a more representative test standard that considers both linear and angular kinematics is to be developed for a guided drop tower.

The key findings of this thesis were:

- A guided drop tower can replicate the linear and angular acceleration of a surrogate in unhelmeted frontal impacts up to 3.00 m/s.
- Although capable of reproducing a resultant peak kinematic response to a falling surrogate the guided drop tower yields angular component responses that differ in direction and time instance.
- In a few selected test cases ballast mass was able to achieve an equivalent peak angular velocity between the drop tower similar and the full-surrogate. However, in general, the use of ballast mass was not able to achieve an equivalent peak angular velocity due to the constraints to the degrees of freedom on the guided drop tower.
- We speculate that differences in helmet liner compression exist between a guided drop tower and a full-surrogate model, and the addition of carriage mass does not achieve equal liner compression in all use cases for helmeted impacts up to 4.50m/s.

6.2 Contributions

The findings of this work identified that significant differences exist between guided drop towers and a fall from height. Most notably the helmeted impact study found that a drop tower significantly overestimates helmet performance in shallow angle impacts due to the constraints imparted by the drop tower and differences in helmet liner engagement relative to a full-surrogate in 4.50m/s falls. Conversely, the drop tower underestimates helmet performance in steep angle impacts at 4.50m/s. This suggests that the drop tower, in its current form, provides a varying estimate of helmet performance dependent on impact angle and in either case does not provide a close approximation of an actual fall. As such, helmet performance inferred by a full-surrogate should not be directly compared to helmet performance inferred by a drop tower.

The identification of the causes of these kinematic differences between the equipment used to evaluate protective headgear and an actual fall from height is a significant contribution toward the advancement of protective headgear's ability to reduce the risk of mTBI. For a new test standard that uses a more representative impact velocity, the significant variance in peak kinematics across impact angles, due to differences in helmet liner engagement and test constraints, needs to be of primary focus to ensure that helmets are evaluated in a way that effectively tests the helmet's impact-attenuating abilities in an actual fall. To address these kinematic differences continued efforts should be focused on achieving drop tower motion that is equivalent to a falling person, if direction and time instance is deemed critical, through the introduction of additional degrees of freedom to the drop tower mechanism. Finally, further work on the use of ballast mass, should be investigated as the drop tower results showed that changing carriage mass in certain use cases can achieve equivalent peak kinematic measures. Used in conjunction, these two alterations may lead to a drop tower impact that is a direct representation of a fall from height that can be used to establish test criteria that ensures the next generation of protective headgear provides enhanced protection from fall induce mTBI.

Bibliography

[1] T. R. Frieden, R. Ikeda, and R. C. Hunt, “Traumatic Brain Injury in the United States,” p. 74.

[2] “TBI_Report_to_Congress_Epi_and_Rehab-a.pdf.” Accessed: Nov. 14, 2022. [Online]. Available: https://www.cdc.gov/traumaticbraininjury/pdf/TBI_Report_to_Congress_Epi_and_Rehab-a.pdf

[3] L.-Z. Kong, R.-L. Zhang, S.-H. Hu, and J.-B. Lai, “Military traumatic brain injury: a challenge straddling neurology and psychiatry,” *Mil. Med. Res.*, vol. 9, no. 1, p. 2, Jan. 2022, doi: 10.1186/s40779-021-00363-y.

[4] L. K. Lindquist, H. C. Love, and E. B. Elbogen, “Traumatic Brain Injury in Iraq and Afghanistan Veterans: New Results from a National Random Sample Study,” *J. Neuropsychiatry Clin. Neurosci.*, vol. 29, no. 3, pp. 254–259, 2017, doi: 10.1176/appi.neuropsych.16050100.

[5] B. McEntire and P. Whitley, “Blunt Impact Performance Characteristics of the Advanced Combat Helmet and the Paratrooper and Infantry Personnel Armor System for Ground Troops Helmet,” p. 39, Aug. 2005.

[6] “ACH PD ar-pd 10-02.pdf.” Accessed: Jan. 25, 2023. [Online]. Available: https://govtribe.com/file/government-file/spm1c111r0118-ach-pd-ar-pd-10-02-dot-pdf

[7] J. R. Crandall *et al.*, “Human surrogates for injury biomechanics research,” *Clin. Anat. N. Y. N*, vol. 24, no. 3, pp. 362–371, Apr. 2011, doi: 10.1002/ca.21152.

[8] NATO, Ed., *Anthropomorphic dummies for crash and escape system testing: = Mannequins anthropométriques utilisés lors des tests d’impact et d’éjection*. in AGARD advisory report, no. 330. Neuilly sur Seine: AGARD, 1996.

[9] B. Chinn *et al.*, “COST 327 Motorcycle Safety Helmets,” *Eur. Comm. Dir. Gen. Energy Transp.*, 2001.

[10] M. Ghajari, S. Peldschus, U. Galvanetto, and L. Iannucci, “Evaluation of the effective mass of the body for helmet impacts,” *Int. J. Crashworthiness*, vol. 16, pp. 621–631, Dec. 2011, doi: 10.1080/13588265.2011.616078.

[11] M. Seidi, M. Memar, and V. Caccese, “Evaluation of effective mass during head impact due to standing falls,” *Int. J. Crashworthiness*, Nov. 2014, doi: 10.1080/13588265.2014.983261.

[12] D. H. Robbins and J. Smrcka, “Review of Dummy Design and Use”.

[13] “FMVSS_571.218 - Motorcycle Helmets 2008 Edition.”

[14] “ECE Reg. 22 Uniform Provisions Concerning the Approval of Protective Helmets and Their Visors for Drivers and Passengers of Motor Cycles and Mopeds.” 2002.

[15] “FMVSS No. 208.” National Highway Traffic Safety Administration.

[16] “Standard Test Method and Equipment used in Evaluating the Performance Characteristics of Protective Headgear/Equipment NOCSAE Doc (ND) 001- 11m12.” 2012.

[17] “CAN-CSA-D113.2-M89 (R2009).” Canadian Standards Association.

[18] “CANCSA-Z263.1-08.pdf.”

[19] “Snell B95A - Standard for Protective Headgear for use with Bicycles.” Snell Memorial Foundations, Jan. 14, 2013. Accessed: Jan. 14, 2013. [Online]. Available: https://www.google.ca/search?q=what+does+astm+stand+for&ie=utf-8&oe=utf-8&aq=t&rls=org.mozilla:en-US:official&client=firefox-a

[20] “Snell Motorcycle M2005.pdf.”
[21] “ND001-11m11-Drop Impact Test Method .pdf.”
[22] E. National Academies of Sciences, H. and M. Division, B. on H. C. Services, and C. on the R. of the D. of V. A. E. for T. B. Injury, *Definitions of Traumatic Brain Injury*. National Academies Press (US), 2019. Accessed: Feb. 24, 2023. [Online]. Available: https://www.ncbi.nlm.nih.gov/books/NBK542588/
[23] D. K. Menon, K. Schwab, D. W. Wright, and A. I. Maas, “Position Statement: Definition of Traumatic Brain Injury,” *Arch. Phys. Med. Rehabil.*, vol. 91, no. 11, pp. 1637–1640, Nov. 2010, doi: 10.1016/j.apmr.2010.05.017.
[24] T. Kay *et al.*, “Definition of mild traumatic brain injury,” *J. Head Trauma Rehabil.*, vol. 8, no. 3, pp. 86–87, 1993.
[25] K.-U. Schmitt, P. F. Niederer, M. H. Muser, and F. Walz, *Trauma Biomechanics: Accidental injury in traffic and sports*. Berlin, Heidelberg: Springer Berlin Heidelberg, 2010. doi: 10.1007/978-3-642-03713-9.
[26] K. Miller, Ed., *Biomechanics of the Brain*. in Biological and Medical Physics, Biomedical Engineering. New York, NY: Springer New York, 2011. doi: 10.1007/978-1-4419-9997-9.
[27] A. M. Nahum and J. W. Melvin, *Accidental Injury: Biomechanics and Prevention*. Springer Science & Business Media, 2012.
[28] “Report to Congress on Traumatic Brain Injury in the United States: Understanding the Public Health Problem among Current and Former Military Personnel,” p. 130.
[29] A. H. S. Holbourn, “Mechanics of Head Injuries,” *The Lancet*, vol. 242, no. 6267, pp. 438–441, Oct. 1943, doi: 10.1016/S0140-6736(00)87453-X.
[30] R. Graham *et al.*, *Neuroscience, Biomechanics, and Risks of Concussion in the Developing Brain*. National Academies Press (US), 2014. Accessed: Feb. 22, 2023. [Online]. Available: https://www.ncbi.nlm.nih.gov/books/NBK185339/
[31] W. N. Hardy, C. D. Foster, M. J. Mason, K. H. Yang, A. I. King, and S. Tashman, “Investigation of Head Injury Mechanisms Using Neutral Density Technology and High-Speed Biplanar X-ray,” *Stapp Car Crash J.*, vol. 45, pp. 337–368, Nov. 2001, doi: 10.4271/2001-22-0016.
[32] A. K. Ommaya and T. A. Gennarelli, “Cerebral concussion and traumatic unconsciousness. Correlation of experimental and clinical observations of blunt head injuries,” *Brain J. Neurol.*, vol. 97, no. 4, pp. 633–654, Dec. 1974, doi: 10.1093/brain/97.1.633.
[33] A. K. Ommaya, R. L. Grubb, and R. A. Naumann, “Coup and contre-coup injury: observations on the mechanics of visible brain injuries in the rhesus monkey,” *J. Neurosurg.*, vol. 35, no. 5, pp. 503–516, Nov. 1971, doi: 10.3171/jns.1971.35.5.0503.
[34] D. Richter, M. P. Hahn, P. A. W. Ostermann, A. Ekkernkamp, and G. Muhr, “Vertical deceleration injuries: a comparative study of the injury patterns of 101 patients after accidental and intentional high falls,” *Injury*, vol. 27, no. 9, pp. 655–659, Nov. 1996, doi: 10.1016/S0020-1383(96)00083-6.
[35] K. G. Warner and R. H. Demling, “The pathophysiology of free-fall injury,” *Ann. Emerg. Med.*, vol. 15, no. 9, pp. 1088–1093, Sep. 1986, doi: 10.1016/S0196-0644(86)80134-2.
[36] D. M. Adamson *et al.*, “Invisible Wounds of War: Psychological and Cognitive Injuries, Their Consequences, and Services to Assist Recovery,” RAND Corporation, Mar. 2008. Accessed: Jan. 24, 2023. [Online]. Available: https://www.rand.org/pubs/monographs/MG720.html

[37] C. W. Hoge, D. McGurk, J. L. Thomas, A. L. Cox, C. C. Engel, and C. A. Castro, “Mild Traumatic Brain Injury in U.S. Soldiers Returning from Iraq,” *N. Engl. J. Med.*, vol. 358, no. 5, pp. 453–463, Jan. 2008, doi: 10.1056/NEJMoa072972.

[38] A. J. MacGregor *et al.*, “Prevalence and psychological correlates of traumatic brain injury in operation iraqi freedom,” *J. Head Trauma Rehabil.*, vol. 25, no. 1, pp. 1–8, 2010, doi: 10.1097/HTR.0b013e3181c2993d.

[39] P. A. Cripton et al., “Bicycle helmets are highly effective at preventing head injury during head impact: Head-form accelerations and injury criteria for helmeted and unhelmeted impacts" Accident Analysis & Prevention, vol. 70, pp. 1-7, 2014, doi: 10.1016/ j.aap.2014.02.016.

[40] D.S. McNally et al., “A computational simulation study of the influence of helmet wearing on head injury risk in adult cyclists" Accident Analysis & Prevention, vol. 60, pp. 15-23, 2013, doi:10.1016/j.aap.2013.07.011.

[41] A. L. Demarco et al., “The impact response of traditional and BMX-style bicycle helmets at different impact severities" Accident Analysis & Prevention, vol. 92, pp. 175-183, 2016, doi: 10.1016/j.aap.2016.03.027.

[42] A. S. McIntosh *et al.*, “Sports helmets now and in the future,” *Br. J. Sports Med.*, vol. 45, no. 16, pp. 1258–1265, Dec. 2011, doi: 10.1136/bjsports-2011-090509.

[43] B. J. McEntire and P. Whitley, “Blunt Impact Performance Characteristics of the Advanced Combat Helmet and the Paratrooper and Infantry Personnel Armor System for Ground Troops Helmet:,” Defense Technical Information Center, Fort Belvoir, VA, Aug. 2005. doi: 10.21236/ADA437530.

[44] “CEMM > Programs > Traumatic Brain Injury > Mild TBI/Concussion > Long-Term Effects.” Accessed: Feb. 26, 2023. [Online]. Available: https://www.cemm.af.mil/Programs/Traumatic-Brain-Injury/Mild-TBI-Concussion/Long-Term-Effects/

[45] J. A. Newman, “Head Injury Criteria in Automotive Crash Testing,” *SAE Trans.*, vol. 89, pp. 4098–4115, 1980.

[46] L. F. Gabler, J. R. Crandall, and M. B. Panzer, “Assessment of Kinematic Brain Injury Metrics for Predicting Strain Responses in Diverse Automotive Impact Conditions,” *Ann. Biomed. Eng.*, vol. 44, no. 12, pp. 3705–3718, Dec. 2016, doi: 10.1007/s10439-016-1697-0.

[47] C. W. Gadd, “Use of a Weighted-Impulse Criterion for Estimating Injury Hazard,” presented at the 10th Stapp Car Crash Conference (1966), Feb. 1966, p. 660793. doi: 10.4271/660793.

[48] J. A. Newman, “The Influence of Time Duration as a Failure Criterion in Helmet Evaluation,” *SAE Trans.*, vol. 91, pp. 3424–3430, 1982.

[49] J. Versace, “A Review of the Severity Index,” SAE International, Warrendale, PA, SAE Technical Paper 710881, Feb. 1971. doi: 10.4271/710881.

[50] L. F. Gabler, J. R. Crandall, and M. B. Panzer, “Development of a Second-Order System for Rapid Estimation of Maximum Brain Strain,” *Ann. Biomed. Eng.*, vol. 47, no. 9, pp. 1971–1981, Sep. 2019, doi: 10.1007/s10439-018-02179-9.
[51] C. Got, A. Patel, and G. Walfisch, “Measured Physical Parameters”.
[52] E. S. Gurdjian, V. L. Roberts, and L. M. Thomas, “Tolerance Curves of Acceleration and Intracranial Pressure and Protective Index in Experimental Head Injury,” *J. Trauma Acute Care Surg.*, vol. 6, no. 5, p. 600, Sep. 1966.
[53] “tp-208-14_tag.pdf.” Accessed: Feb. 21, 2023. [Online]. Available: https://www.nhtsa.gov/sites/nhtsa.gov/files/documents/tp-208-14_tag.pdf
[54] H. Kimpara, Y. Nakahira, M. Iwamoto, S. Rowson, and S. Duma, “Head Injury Prediction Methods Based on 6 Degree of Freedom Head Acceleration Measurements during Impact,” *Int. J. Automot. Eng.*, vol. 2, pp. 13–19, 2011.
[55] “Diffuse Axonal Injury: An Important Form of Traumatic Brain Damage.” Accessed: Feb. 14, 2023. [Online]. Available: https://journals.sagepub.com/doi/epdf/10.1177/107385849800400316
[56] A. M. Bailey *et al.*, “Comparison of Laboratory and On-Field Performance of American Football Helmets,” *Ann. Biomed. Eng.*, vol. 48, no. 11, pp. 2531–2541, Nov. 2020, doi: 10.1007/s10439-020-02627-5.
[57] R. M. Greenwald, J. T. Gwin, J. J. Chu, and J. J. Crisco, “Head Impact Severity Measures for Evaluating Mild Traumatic Brain Injury Risk Exposure,” *Neurosurgery*, vol. 62, no. 4, p. 789, Apr. 2008, doi: 10.1227/01.neu.0000318162.67472.ad.
[58] J. R. Crandall *et al.*, “Human surrogates for injury biomechanics research,” *Clin. Anat.*, vol. 24, no. 3, pp. 362–371, Apr. 2011, doi: 10.1002/ca.21152.
[59] J. K. Foster, J. O. Kortge, and M. J. Wolanin, “Hybrid III—A Biomechanically-Based Crash Test Dummy,” *SAE Trans.*, vol. 86, pp. 3268–3283, 1977.
[60] S. MacGillivray, G. Wynn, M. Ogle, J. Shore, J. P. Carey, and C. R. Dennison, “Repeatability and Biofidelity of a Physical Surrogate Neck Model Fit to a Hybrid III Head,” *Ann. Biomed. Eng.*, vol. 49, no. 10, pp. 2957–2972, Oct. 2021, doi: 10.1007/s10439-021-02786-z.
[61] T. Whyte *et al.*, “A Review of Impact Testing Methods for Headgear in Sports: Considerations for Improved Prevention of Head Injury Through Research and Standards,” *J. Biomech. Eng.*, vol. 141, no. 7, p. 070803, Jul. 2019, doi: 10.1115/1.4043140.
[62] R. Butz, B. Knowles, J. Newman, and C. Dennison, “Effects of external helmet accessories on biomechanical measures of head injury risk: an ATD study using the HybridIII headform,” *J. Biomech.*, vol. 48, no. 14, pp. 3816–3824.
[63] H. Y. Yu, “A Laboratory Study on the Effect of Helmet Fit on Biomechanical Measures of Head and Neck Injury in Simulated Impact”.
[64] E. Bliven *et al.*, “Evaluation of a novel bicycle helmet concept in oblique impact testing,” *Accid. Anal. Prev.*, vol. 124, pp. 58–65, Mar. 2019, doi: 10.1016/j.aap.2018.12.017.
[65] D. Stitt, N. Kabaliuk, K. Alexander, and N. Draper, “Drop Test Kinematics Using Varied Impact Surfaces and Head/Neck Configurations for Rugby Headgear Testing,” *Ann. Biomed. Eng.*, vol. 50, no. 11, pp. 1633–1647, 2022, doi: 10.1007/s10439-022-03045-5.
[66] “dot_218_testprocedure.pdf.” Accessed: Jan. 25, 2023. [Online]. Available: https://smf.org/standards/pdf/dot_218_testprocedure.pdf

[67] “ND002-17m21-NOCSAE-Football-Helmet-Performance-Specfication.pdf.” Accessed: Jan. 05, 2023. [Online]. Available: https://nocsae.org/wp-content/uploads/2018/05/ND002-17m21-NOCSAE-Football-Helmet-Performance-Specfication.pdf
[68] “M2020_Final.pdf.” Accessed: Jan. 25, 2023. [Online]. Available: https://smf.org/standards/m/2020/M2020_Final.pdf
[69] H. S. Philo, P. Appel, and E. B. Becker, “William C. Chilcott, Ph.D. Channing L. Ewing, M.D. Harold A. Fenner, Jr., M.D., President Richard G. Snyder, Ph.D. Daniel J. Thomas, M.D.”.
[70] “EN 1078 (1997) Pedal Cyclists Skateboards and Roller Skates.pdf.”
[71] “EN 14572:2005 - High Performance Helmets for Equestrian Activities,” iTeh Standards. Accessed: Jan. 25, 2023. [Online]. Available: https://standards.iteh.ai/catalog/standards/cen/fa00d64d-9c23-4542-bc35-8911591b6bfc/en-14572-2005
[72] “1995-Performance Specification Helmet, Ground Troops And Parachutists for the canadian forces L1939SPEC.”
[73] “fmvss218.htm.” Accessed: Feb. 09, 2023. [Online]. Available: https://one.nhtsa.gov/people/injury/pedbimot/NoMigrate/fmvss218.htm
[74] C. on R. of T. P. U. by the D. to T. CombatHelmets, B. on A. S. and Technology, D. on E. and P. Sciences, and N. R. Council, *Characterization Tests for the Advanced Combat Helmet and Future Helmets*. National Academies Press (US), 2014. Accessed: Jan. 25, 2023. [Online]. Available: https://www.ncbi.nlm.nih.gov/books/NBK224904/
[75] Society of Automotive Engineers, “SAE J211 Instrumentation for Impact Test - Part 1: Electronic Instrumentation.” SAE International, 2014. [Online]. Available: https://saemobilus.sae.org/content/j211/1_201403
[76] A. J. Padgaonkar, K. W. Krieger, and A. I. King, “Measurement of Angular Acceleration of a Rigid Body Using Linear Accelerometers,” *J. Appl. Mech.*, vol. 42, no. 3, pp. 552–556, Sep. 1975, doi: 10.1115/1.3423640.
[77] A. M. Hering and S. Derler, “Motorcycle Helmet Drop Tests Using a Hybrid Iii Dummy,” 2000.
[78] *Manuals Combined: 30+ Army Navy And Air Force Aviation EJECTION SEAT Studies*. Jeffrey Frank Jones.
[79] “1998_cpsc_a_addendum_to_b95.pdf.” Accessed: Jan. 25, 2023. [Online]. Available: https://smf.org/standards/pdf/1998_cpsc_a_addendum_to_b95.pdf
[80] K. Turgut, M. E. Sarihan, C. Colak, T. Güven, A. Gür, and S. Gürbüz, “Falls from height: A retrospective analysis,” *World J. Emerg. Med.*, vol. 9, no. 1, pp. 46–50, 2018, doi: 10.5847/wjem.j.1920-8642.2018.01.007.
[81] National Research Council (U.S.), *Review of Department of Defense Test Protocols for Combat Helmets*. Washington, D.C.: National Academies Press, 2014. [Online]. Available: https://login.ezproxy.library.ualberta.ca/login?url=https://search.ebscohost.com/login.aspx?direct=true&db=nlebk&AN=867835&site=eds-live&scope=site
[82] “CSA CAN/CSA-D113.2-M89 - Cycling Helmets.” Accessed: Oct. 31, 2021. [Online]. Available: https://ewb-ihs-com.login.ezproxy.library.ualberta.ca/#/document/WLVCDFAAAAAAAAAA?sr=qt-1-8&kbid=4,5%7C20027&docid=942906693#hebb9f2da

[83] L. M. Lix, J. C. Keselman, and H. J. Keselman, “Consequences of Assumption Violations Revisited: A Quantitative Review of Alternatives to the One-Way Analysis of Variance ‘F’ Test,” *Rev. Educ. Res.*, vol. 66, no. 4, pp. 579–619, 1996, doi: 10.2307/1170654.
[84] M. J. Blanca, R. Alarcón, and J. Arnau, “Non-normal data: Is ANOVA still a valid option?,” *Psicothema*, no. 29.4, pp. 552–557, Nov. 2017, doi: 10.7334/psicothema2016.383.
[85] E. Schmider, M. Ziegler, E. Danay, L. Beyer, and M. Bühner, “Is it really robust? Reinvestigating the robustness of ANOVA against violations of the normal distribution assumption,” *Methodol. Eur. J. Res. Methods Behav. Soc. Sci.*, vol. 6, no. 4, pp. 147–151, 2010, doi: 10.1027/1614-2241/a000016.
[86] J. Shin *et al.*, *Biofidelity Evaluation of the Hybrid-III 50th Male and the THOR-50M in Reclined Frontal Impact Sled Tests*. 2022.